UPPSALA
UNIVERSITET

Digital Comprehensive Summaries of Uppsala Dissertations from the Faculty of Pharmacy 269

Ligands of the Angiotensin II Type 2 Receptor

Exploring structure and function of the AT_2R ligand C38

REBECKA ISAKSSON

ACTA
UNIVERSITATIS
UPSALIENSIS
UPPSALA
2019

ISSN 1651-6192
ISBN 978-91-513-0630-8
urn:nbn:se:uu:diva-381102

Dissertation presented at Uppsala University to be publicly examined in Room A1:107a, BMC, Husargatan 3, Uppsala, Wednesday, 29 May 2019 at 13:15 for the degree of Doctor of Philosophy (Faculty of Pharmacy). The examination will be conducted in English. Faculty examiner: Associate Professor Annette Bayer (Department of Chemistry, University of Tromsø).

Abstract
Isaksson, R. 2019. Ligands of the Angiotensin II Type 2 Receptor. Exploring structure and function of the AT_2R ligand C38. *Digital Comprehensive Summaries of Uppsala Dissertations from the Faculty of Pharmacy* 269. 74 pp. Uppsala: Acta Universitatis Upsaliensis.
ISBN 978-91-513-0630-8.

The renin-angiotensin-aldosterone-system (RAAS) control blood-pressure regulation, exerted by the main effector peptide angiotensin II (AngII) binding the angiotensin II type 1 receptor (AT_1R). While hypertension is the most known disease caused by over-activity in RAAS, several proteins in the system exhibit protective functions.

One of these protective proteins is the GPCR angiotensin II type 2 receptor (AT_2R). After decades of research its biological role remain to be fully elucidated, exemplified by the two AT_2R ligands currently in clinical trials; agonist C21 for treatment of idiopathic pulmonary fibrosis, and antagonist EMA401 for treatment of peripheral neuropathic pain. Making a minor structural change in C21 shifted the pharmacological profile, generating the regioisomer antagonist C38. The renewed interest in AT_2R antagonists as potential drugs to treat neuropathic pain make continued studies of antagonist C38 highly interesting.

The aim of this thesis was to continue exploring the structure-activity relationship of antagonist C38 by investigating three chemical motifs to identify compounds with better drug-like properties. Developing a new chemical method, transesterification of sulfonyl carbamates, allowed quick modification of one of the motifs. Reducing the length of the sulfonyl carbamate chain significantly increased metabolic stability in liver microsomes without losing affinity for AT_2R. Using a model substrate, the transesterification reaction was applied in a microwave heated continuous-flow system.

Adding small substituents to the central phenyl ring generated a second library of ligands with retained affinity, but with no observed increase in metabolic stability. Docking studies with this library and a recently presented crystal structure of AT_2R, resulted in a proposed binding mode of C38. Replacing the imidazole head group with bicyclic amides slightly improved affinity. While metabolic stability improved compared to previously published amide analogs, the bicyclic ligands were inferior to C38. Developing an assay based on RAW264.7 macrophages allowed a new evaluation of the functional activity exhibited by C38. In contrast to previous research, C21 and C38 both display agonistic functional activity in the macrophage assay.

In summary, the work presented in this thesis expand the structure-activity relationship of C38 and its pharmacological profile. Two new ligands were identified that could serve as tools in murine models of neuropathic pain.

Keywords: Angiotensin II type 2 receptor, AT2R antagonists, sulfonyl carbamates, bicyclic amides, metabolic stability, functional activity assay, pharmacological profile, medicinal chemistry, structure-activity relationship

Rebecka Isaksson, Department of Medicinal Chemistry, Preparative Medicinal Chemistry, Box 574, Uppsala University, SE-751 23 Uppsala, Sweden.

ISSN 1651-6192
ISBN 978-91-513-0630-8
urn:nbn:se:uu:diva-381102 (http://urn.kb.se/resolve?urn=urn:nbn:se:uu:diva-381102)

To Marie, Betty, Emmeline, Ellen, Sonja, Fredrika, Agnes,
and all the others who came before me
and made this possible

List of Papers

The following papers form the basis of this thesis, referenced in the text by their Roman numerals.

I Isaksson, R., Kumpiņa, I., Larhed, M., Wannberg, J. (2016) Rapid and straightforward transesterification of sulfonyl carbamates. *Tetrahedron Lett.*, 57(13):1476-1478

II Kumpiņa, I., Isaksson, R., Sävmarker, J., Wannberg, J., Larhed, M. (2016) Microwave Promoted Transcarbamylation Reaction of Sulfonylcarbamates under Continuous-Flow Conditions. *Org. Process Res. Dev.*, 20(2):440-445

III Wannberg, J., Isaksson, R., Bremberg, U., Backlund, M., Sävmarker, J., Hallberg, M., Larhed, M. (2018) A convenient transesterification method for synthesis of AT2 receptor ligands with improved stability in human liver microsomes. *Bioorg. Med. Chem. Lett.*, 28(3):519-522

IV Isaksson, R., Lindman, J., Sallander, J., Wannberg, J., Backlund, M., Baraldi, D., Widdop, R., Hallberg, M., Åqvist, J., Gutiérrez-de-Terán, H., Gising, J., Larhed, M. A Series of Analogues to the AT2R Prototype Antagonist C38 Allow Fine Tuning of the Previously Reported Antagonist Binding Mode. *ChemistryOPEN*, 8(1):114-125

V Isaksson, R., Casselbrant, A., Elebring, E., Hallberg, M., Larhed, M., Fändriks, L. Direct Stimulation of Angiotensin II Type 2 Receptor Reduce Nitric Oxide Production in Lipopolysaccharide Treated RAW264.7 Mouse Macrophages. *Manuscript.*

Contents

Introduction 11
G-Protein Coupled Receptors 12
The Renin-Angiotensin-Aldosterone System 13
Drugs Acting on the Renin-Angiotensin-Aldosterone System 14
Angiotensin II Type 2 Receptor 15
Neuropathic Pain and the Role of AT_2R 17
Recently Discovered Proteins in RAAS 17
Development of AT_2R Ligands **C21** and **C38** 18

Aims 20

Transesterification of Sulfonyl Carbamates and the Applicability of Microwave Heated Continuous-Flow (Paper I and II) 21
Background and Strategy 21
Microwave Heated Continuous-Flow 22
Reaction Scope in Batch Mode 23
Reaction Scope in a Continuous-Flow System 25
Application to Biologically Relevant Compounds 29
Summary and Future Outlook 30

Structure-Activity Investigation of **C38**, a Reported AT_2R Antagonist (Papers III and IV) 31
Background 31
Synthesis and Evaluation of Sulfonyl Carbamate Analogues (Paper III) 33
Strategy 33
Synthetic Work 33
Results and Discussion 36
Synthesis and Evaluation of Phenyl-Ring Derivatives (Paper IV) 38
Strategy 38
Synthetic Work 38
Results and Discussion 39
Synthesis and Evaluation of Bicyclic Analogues (Paper IV) 43
Strategy 43
Synthetic Work 43
Results and Discussion 45

Supplementary In Vitro Pharmacology 47
Summary of the Structure-Activity Studies of **C38** and Future Outlook 48

Investigation of NO release in Macrophages as a Functional Activity Indicator for AT_2R Ligands (Paper V) 50
Background and Strategy 50
Macrophages and AT_2R 50
Cell Validation and Basal Protein Expression 52
Evaluating the Assay with AT_2R Ligands **C21** and **C38** 53
Effect of AT_2R Ligands **C21** and **C38** in LPS-Differentiated Macrophages 53
Effect of **C21** on Macrophages During Simultaneous Macrophage Differentiation 55
Effect of AT_2R Ligands **C21** and **C38** in Highly Stimulated Macrophages 56
Summary and Future Outlook 58

Concluding Remarks 60

Populärvetenskaplig Sammanfattning 62

Acknowledgments 65

References 66

Abbreviations

AAM	Alternatively activated macrophages
ACE (/2)	Angiotensin-converting enzyme (/2)
ADME	Absorption, distribution, metabolism, excretion
Ala	Alanine
Ang_{1-7}	Angiotensin 1-7
Ang_{1-9}	Angiotensin 1-9
AngII	Angiotensin II
ANOVA	Analysis of variance
ARBs	Angiotensin-receptor blockers
Arg	Arginine
Asp	Aspartic acid
AT_1R	Angiotensin II type 1 receptor
AT_2R	Angiotensin II type 2 receptor
BPR	Back-pressure regulator
CAM	Classically activated macrophages
CYP (/450)	Cytochrome P450
DCM	Dichloromethane
DIPEA	*N*,*N*-Diisopropylethylamine
DME	Dimethoxyethane
DMF	Dimethylformamide
DMSO	Dimethyl sulfoxide
DNA	Deoxyribonucleic acid
DRG	Dorsal-root ganglion
eNOS	Endothelial nitric oxide synthase
GAPDH	Glyceraldehyde 3-phosphate dehydrogenase
GPCR	G-protein coupled receptor
HAEC	Human aortic endothelial cells
HIV	Human immunodeficiency virus
His	Histidine
HLM	Human liver microsomes
HPLC	High performance liquid chromatography
IC_{50}	Inhibitor concentration giving 50% inhibition
INF-γ	Interferon-gamma
IL	Interleukin
iNOS	Inducible nitric oxide synthase
Ile	Isoleucine

K_i	Inhibition constant
KS	Kinetic solubility
LC	Liquid chromatography
Leu	Leucine
LPS	Lipopolysaccharide
M1	Pro-inflammatory macrophages
M2	Anti-inflammatory macrophages
MeCN	Acetonitrile
MIDA	*N*-Methyliminodiacetic acid
MLM	Mouse liver microsomes
MS	Mass spectroscopy
MW	Microwave
NF-κβ	Nuclear factor κβ
NMR	Nuclear magnetic resonance
Phe	Phenylalanine
Pro	Proline
RAAS	Renin-angiotensin-aldosterone system
RNS	Reactive nitrogen species
ROS	Reactive oxygen species
r.t.	Room temperature
Sar	Sarcosine
SEM	Standard error of mean
TEA	Triethylamine
TFA	Trifluoroacetic acid
THF	Tetrahydrofuran
TLR4	Toll-like receptor 4
TNF-α	Tumor necrosis factor α
TRPA1	Transient receptor potential ankyrin 1
Tyr	Tyrosine
UV	Ultraviolet
Val	Valine

Introduction

Medicinal chemistry is an integral part of modern drug discovery and development. Simplified, the process is often outlined as linear (Figure 1) although, in reality developing pharmaceutical agents frequently constitute several iterative, connected processes. In the early days of drug discovery, chemistry was often considered the key discipline, and synthesized agents formed the starting point for many research projects. During the past decades, drug discovery has increasingly started with efforts to understand the biological cause of a disease. After identifying the potential biological target, the work of evaluating and synthesizing possible ligands binding that target commence. In the interdisciplinary field of medicinal chemistry, available biological data is used to drive the design and synthesis of compound libraries that eventually (and hopefully) result in a candidate drug.[1]

Drug discovery and development is costly and time consuming. A recent report by DiMasi et al. estimate the total cost of developing a drug from bench to market has increased to $2.6 billion.[2] As the drug discovery and development process proceeds, a large number of starting compounds (5 000-10 000) decrease to only a few lead compounds, and eventually one candidate drug is selected (Figure 1). The clinical trials are the most costly part of the drug discovery process and are also associated with the highest attrition rate.[1–5]

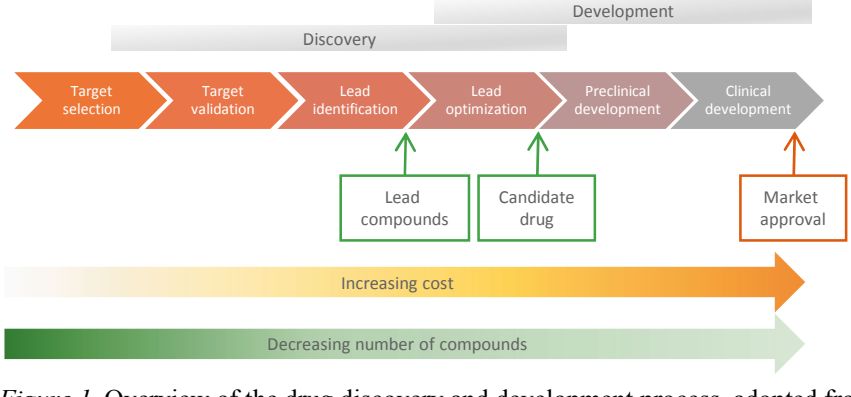

Figure 1. Overview of the drug discovery and development process, adopted from Rang and Hill 2013.[1]

A vast majority of marketed pharmaceutical agents act on human targets, while drugs acting on infecting organisms or other miscellaneous agents (vitamins, inorganic salts, plasma substitutes and similar) make up only about a fourth of all therapeutic drugs.[1] The large majority of druggable biological targets are membrane bound proteins such as receptors, enzymes, ion channels, or transport proteins. There are also intracellular targets however, due to their challenging location only a smaller portion of marketed drugs interacts with such targets.

G-Protein Coupled Receptors

G-protein coupled receptors (GPCR) are one of the largest families of proteins in the mammalian genome and are fundamental in physiological function. Signal transduction is mediated when the membrane-bound GPCRs interact with hormones, peptides, neurotransmitters, and other extracellular cues, an interaction that cause intracellular responses. The receptors have been extensively studied due to their druggable extracellular sites, and their involvement in pathophysiology. Recent estimates indicate a third of all currently marketed drugs interact with a GPCR.[6] A GPCR consist of seven membrane-spanning helices, and interact with a G-protein in the intracellular domain. The vertebra GPCRs are commonly divided into five families according to the GRAFS classification: ***g***lutamate, ***r***hodopsin, ***a***dhesion, ***f***izzled/taste 2, and ***s***ecretin.[7] The largest family by far is the rhodopsin-superfamily, and understandably most of the drugs targeting GPCRs act on receptors in this family.

In the classical description, the GPCR equilibrates between active and inactive states, and the ligands binding it will stabilize one of these states. The agonist will stabilize an active conformation and thus, shift the equilibrium to the fully active state (Figure 2). Partial agonists will also bind an active state of the GPCR but will only shift the equilibrium partly, and hence exhibiting a lower activation of the GPCR as opposed to full agonists. An inverse agonist will stabilize an inactive state, shifting the equilibrium to the inactive side and lowering the basal activity of the GPCR. Neutral antagonists will competitively inhibit the agonist action without affecting the equilibrium and thus, prevent the active state while not altering the basal activity.[8,9] Both inverse agonist and partial agonist present as useful in drug discovery. If an inverse agonist shift the equilibrium of active and inactive states, which an antagonist do not, an inverse agonist should be able to reverse the pathophysiological activation causing a disease. A partial agonist can act as competitive antagonist but rather than blocking the receptor's signaling, the ligand will normalize the signal transduction.

Evidence of other more complex GPCR behavior has expanded the presented model. GPCRs do not only interact with G-proteins in signal

transduction, and biased activation can shift which intracellular pathway is activated. Further, GPCRs can internalize and partake in intracellular activation, as well as interact with other GPCRs via both homo- and heterodimerization. In these dimeric states, a GPCR can exert a functional activity on its partner GPCR depending on which ligand it binds.[9–12]

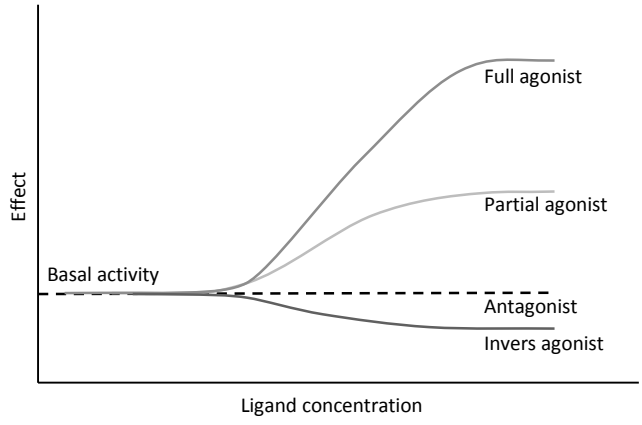

Figure 2. Classical description of the effect a ligand has on GPCR signaling.

The Renin-Angiotensin-Aldosterone System

In the body, the renin-angiotensin-aldosterone system (RAAS) regulate blood pressure and fluid electrolyte balance. There are several marketed pharmaceutical agents, as well as candidate drugs, that target proteins in RAAS. The discovery of the enzymatic cascade that constitutes the hormone system RAAS begun in the 1890s when renin was first isolated from kidney extracts.[13,14] In the 1930s, scientists concluded that renin is an enzyme catalyzing the formation of angiotensin (I).[15] Two decades later the discovery of angiotensin-converting enzyme (ACE) led to the identification of angiotensin II (AngII), which is the key mediator in blood-pressure regulation.[13,16,17] In RAAS, the kidneys control release of renin to the central circulation where the enzyme catalyzes the conversion of the hepatically derived angiotensinogen into angiotensin I (Figure 3). ACE will cleave the two C-terminal amino acids from the inactive decapeptide, generating the major effector peptide AngII. If RAAS becomes over-active, the result will be hypertension and various cardiovascular diseases (i.e. congestive heart failure, coronary ischemia, and renal insufficiency).[13,18] The hypertensive effect of AngII was determined in the mid-1970s[19–21] using the AngII-analog Saralasin (Sar^1Ala^8-AngII). Parallel to this, the GPCR that binds AngII and exerts the hypertensive effect of RAAS was discovered, the angiotensin II type 1 receptor (AT_1R).

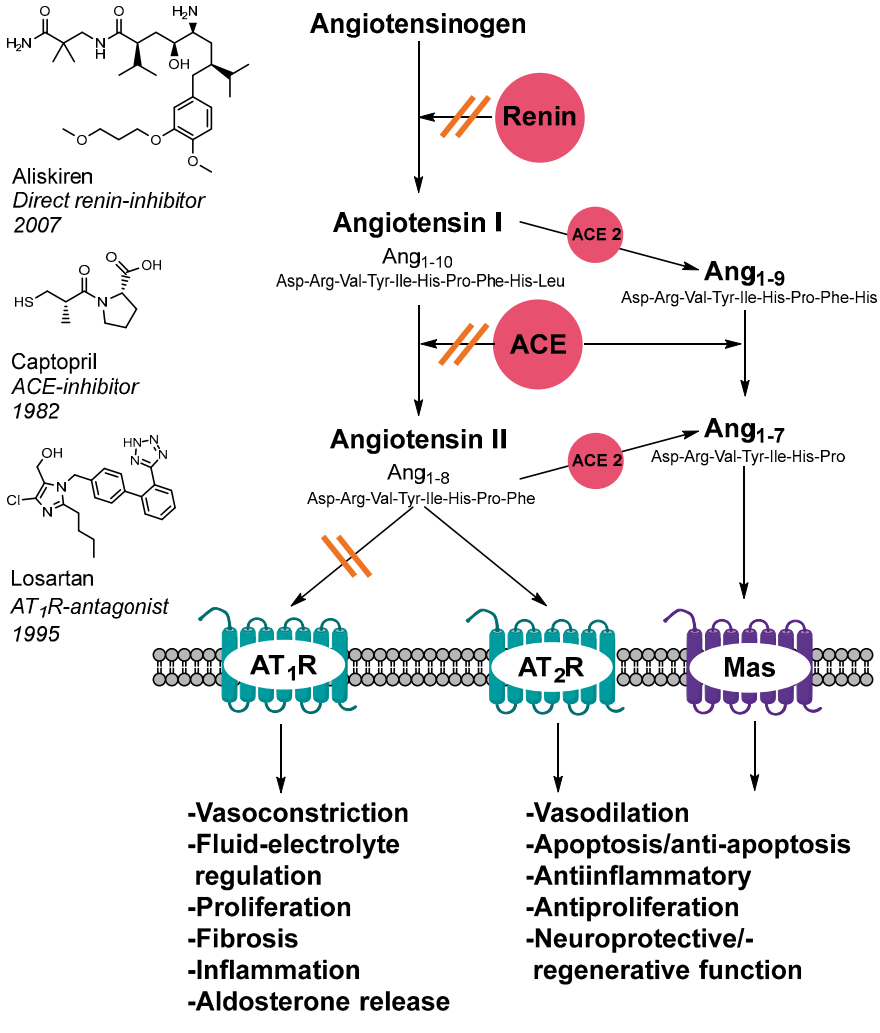

Figure 3. Overview of the RAAS cascade leading to the formation of the main effector peptide AngII, the proteins the peptide bind and their effects. The orange lines indicate the pathways blocked by anti-hypertensive drugs on the market. The recently discovered Ang_{1-7} and receptor Mas pathway is also included. Adapted from Unger et al. 2015.[22]

Drugs Acting on the Renin-Angiotensin-Aldosterone System

Inhibitors of the two proteases important for forming AngII (renin and ACE) or antagonists of AT_1R are well established therapeutics (Figure 3). The first anti-hypertensive drug reaching the market that targeted a protein in RAAS was the ACE-inhibitor captopril in 1982.[23,24] In 1995, losartan was approved for marketing and was the first drug targeting AT_1R as a treatment of hypertension.[25,26] Several additional ACE-inhibitors and angiotensin-receptor

blockers (ARBs, or sartans) have since been presented and these drugs are extensively used to treat hypertension.

Since the discovery of the enzyme renin, it has been proposed as a target for the treatment of hypertension. After decades of research the first, and to date only, renin-inhibitor aliskiren was approved for the market in 2007. The inhibition occurs early in the RAAS cascade and was proposed to provide a broader protection against the cardiovascular effects exerted by RAAS. Several studies have concluded that the effect of aliskiren alone is low and hence, the drug is commonly used in combination with other anti-hypertensive treatments.[27,28]

Angiotensin II Type 2 Receptor

In the late 1980s evidence emerged of a second receptor binding AngII, the angiotensin II type 2 receptor (AT_2R, Figure 3)[29,30], disrupting the previous picture of the RAAS. The discovery led to extensive discussions on both the existence and function of AT_2R. The GPCR earned the epithet "enigmatic", relating to its constitutive action and atypical intracellular signaling pathways.[22,31] The human AT_2R shares 30% sequence identity with human AT_1R, both belonging to the rhodopsin γ-family[32,33], and in the genome AT_2R is located on the X chromosome.[34]

The expression of AT_2R in healthy tissue is low and the receptor often counteract the effects of AT_1R. Data indicate AT_2R is important in fetal development, as the receptor is predominantly expressed in fetal tissue.[35,36] In adults, AT_2R is mainly expressed in the uterus, adrenal gland, smooth muscle, heart, and kidney.[37,38] Notably, AT_2R is strongly upregulated following tissue damage,[39,40] such as vascular[41] and neuronal injury[42], brain ischemia[43], and myocardial infarction[44–46]. Studies have proposed AT_2R is involved in wound healing and tissue repair[47,48], mediate cell differentiation and apoptosis[49–51], display bot anti-inflammatory and neuroprotective propoerties[52–55], and exert an AT_1R opposing vasodilating effect[56,57].

In recent years AT_2R has emerged as a promising new drug target in the protective arm of RAAS, although the question as to whether to block or activate the GPCR remains unanswered.[22,58–60] During the past decade, four AT_2R ligands of varied functional activity have entered clinical trials for different indications. Mitsubishi Tanabe Pharma developed the AT_2R agonist MP-157 as a potential treatment for hypertension.[61] The compound entered phase I clinical trials but was discontinued in 2018. Lanthio Pharma has developed another AT_2R agonist, lanthipeptide MOR107 that entered phase I clinical trials in 2017 for the indication diabetic nephropathy and fibrosis.[62] Since this, the compound has returned to preclinical investigations focused on oncology. The Vicore Pharma AT_2R agonist **C21** (Figure 4), developed by the Hallberg research group at Uppsala University in 2004[63], has gone through

phase I clinical trials. The compound is currently undergoing phase II clinical trials as a possible treatment for idiopathic pulmonary fibrosis, following successful preclinical studies in mice.[64] The fourth AT_2R ligand to enter clinical trials is the antagonist **EMA401** as a proposed treatment of peripheral neuropathic pain (Figure 4).[65–67]

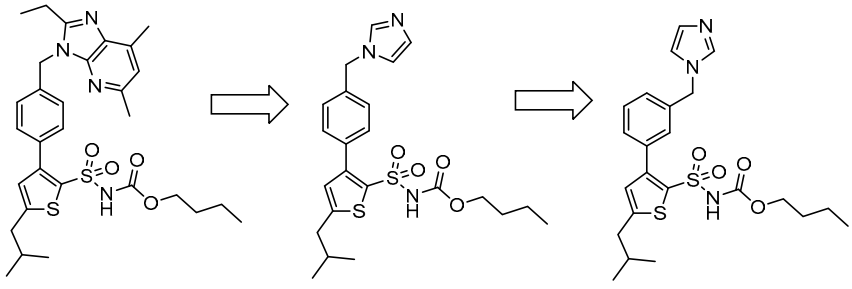

L-162,313
K_i (nM)
AT_1R (rat) = 3.9
AT_2R (pig) = 2.8
Agonist (AT_2R / AT_1R)

C21
K_i (nM)
AT_1R (human) > 10 000
AT_2R (human) = 1.1
AT_2R (pig) = 0.4
Agonist (AT_2R)

C38
K_i (nM)
AT_1R (human) > 10 000
AT_2R (human) = 270
AT_2R (pig) = 19
Antagonist (AT_2R)

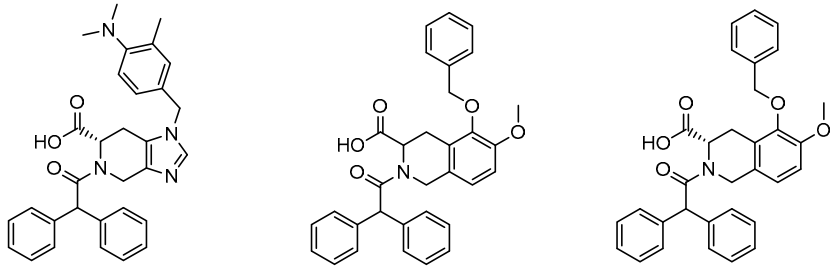

PD123,319
IC_{50} (nM)
AT_1R (rat) > 10 000
AT_2R (rat) = 34
Antagonist (AT_2R)

PD126,055 (EMA400)
IC_{50} (nM)
AT_1R (human) = 2 918
AT_2R (human) = 75
Antagonist (AT_2R)

EMA401
IC_{50} (nM)
AT_1R (human) = 408
AT_2R (human) = 39
Antagonist (AT_2R)

Figure 4. The first reported non-peptide ligand binding AT_2R **L-162,313**, led to the discovery of the first reported selective AT_2R agonist **C21**.[63,68] Further studies revealed the structurally related AT_2R selective antagonist **C38**.[69,70] The established prototype antagonist **PD123,319** was discovered in the mid-1990s, along with **PD126,055** (**EMA400**).[66,71–74] The *S*-enantiomer of the latter is **EMA401** that recently entered phase IIb clinical trials as a potential pharmaceutical agent to treat peripheral neuropathic pain.[67]

Neuropathic Pain and the Role of AT_2R

Neuropathic pain is defined as pain arising due to pathology afflicting the somatosensory system. It is caused by lesions or disease (e.g. viruses such as herpes or HIV, diabetes, cancer, etc.) affecting the central and/or peripheral nervous system.[75] Epidemiological research indicate the prevalence of chronic pain with neuropathic character is 7-10% in the general population.[76,77] The prevalence in specific patient groups is much higher; studies among diabetics indicate 16-23 % suffer from diabetic neuropathy.[78,79] Presently, neuropathic pain is undermanaged due to the lack of efficacious pharmacological treatment. The debilitating condition often have a large negative effect on the quality of life, and identifying the correct treatment for patients is challenging due to the variation in the underlying causes and symptoms.[75,80,81]

The heterogeneous etiology of neuropathic pain also make the underlying mechanism difficult to elucidate. Hyperexcitability in dorsal-root ganglion (DRG) neurons is proposed to be a key mechanism contributing to neuropathic pain. Recent in vitro studies using both cultured cells of neuronal origin and cultured adult rat DRG neurons indicate AngII can induce neuronal excitability. In the same studies the AT_2R antagonist **EMA401** reported to inhibit this effect.[66,82–84] This ligand is the *S*-enantiomer of the racemic compound **EMA400**, formerly known as the Parke-Davies compound **PD126,055** (Figure 4).[71,72,85] The antagonist **EMA401** was acquired by Novartis from Spinifex Pharmaceuticals Pty Ltd, Australia in 2015. Successful completion of phase IIa clinical trials for post-herpetic neuralgia, validated AT_2R as a target in peripheral neuropathic pain management. In 2018, the phase IIb clinical trials commenced with the indication altered to diabetic neuropathy.[67,85]

Recently Discovered Proteins in RAAS

As outlined in figure 3, the AngII-AT_1R-AT_2R axis is not the only known axis in the RAAS. Since the discovery of the first anti-hypertensive drugs, the complexity of the RAAS has increased and the protective function of RAAS become more apparent.[86] The discovery of angiotensin converting enzyme 2 (ACE2) led to the discovery of both Ang_{1-9} and Ang_{1-7}. ACE2 can catalyze the formation of Ang_{1-9} from angiotensin I, and Ang_{1-7} from AngII. In the presence of Ang_{1-9}, ACE can also generate Ang_{1-7}. The gene encoding the receptor binding Ang_{1-7} was described in the late 1980s, the Mas receptor.[87] Erroneously, the gene *Mas* was first proposed to be an oncogene. However, in 2003 the link between the Mas receptor and Ang_{1-7} was disclosed and since then, the Mas-Ang_{1-7} axis has been recognized as an integral part of the protective arm of RAAS, where the Mas receptor exerts similar effects to the AT_2R.[88,89]

Development of AT_2R Ligands **C21** and **C38**

As previously mentioned, the clinical candidate AT_2R agonist **C21** was presented in 2004[63] and was the first AT_2R selective non-peptide agonist ligand published. Compound **C21** has made a large impact on the research involving AT_2R, and complemented the action of the established AT_2R peptide agonist CGP42112 and the prototype antagonist **PD123,319**. The latter is structurally related to antagonist **PD126,055** (**EMA400**) and was identified at the same time (Figure 4).[71,72,85] Using **C21**, it has been possible to investigate the role of AT_2R in disease development and the protective function of the receptor. In addition, the compound has helped further the understanding of AT_2R signaling pathways.

Compound **C21** is derived from the first reported non-peptide AT_1R agonist, Merck compound **L-162,313** presented in 1995 (Figure 4).[68,90] **L-162,313** exhibits similar affinity for AT_1R as AT_2R acting as an agonist at both receptors.[91] Selectivity for AT_2R over AT_1R was accomplished by replacing the imidazo-pyridine with an imidazole, yielding **C21**. The structure-activity relationship of the **C21** scaffold has since been investigated, and will be briefly summarized below, please see reference 92–94 for reviews.

In the 2004 report, Wan et al. concluded that the size of the scaffold head group is important for AT_2R selectivity. Removing the head group will result in inactive ligands, as will moving the methylene linker which likely position the head group unfavorably.[63] The sulfonyl carbamate moiety in the **C21** scaffold was found to be sensitive to change, as reported by Wu et al. in 2006.[95] Further, the authors found the thiophene ring to be exchangeable with a phenyl ring while maintaining selectivity and reasonable affinity. Additionally, the isobutyl can be slightly altered, although large groups in that position render the compounds inactive. In 2007, Murugaiah et al. briefly explored the phenyl ring finding it could be exchanged with a furan ring without loss of affinity for AT_2R.[96] Replacing the phenyl ring with pyridine or thiophene was not favored. Several series were synthesized attempting to identify a suitable replacement for the imidazole that can interact with and inhibit cytochrome P450 enzymes (CYP450). Two amide series were presented in 2007 and in both series a majority of the ligands generated exhibited significantly reduced AT_2R affinity.[96] The imidazole has also been replaced with various heterocyclic derivatives with varied results. While some compounds were rendered inactive, several exhibited reasonable affinity in comparison to **C21**.[97] In a 2008 paper, Wallinder et al. investigated a third amide series where the methylene linker was removed and thus, moved the amides closer to the phenyl ring. This succeeded in improving affinity, while none of the ligands were as potent as **C21**.[98]

In 2012, Murugaiah et al. presented the antagonist **C38** (Figure 4). In this regioisomer of **C21** the methylene imidazole has been shifted from the para position relative to the thiophene, to the meta position generating compound

C38. This minor structural change altered the pharmacological profile of the ligand, which exhibited antagonistic properties.[69,99] Later studies by Wallinder et al. have suggested it is the relative position of the imidazole head group and the isobutyl substituent on the thiophene ring that is the determinant of a ligand's functional activity.[100] Such small changes can affect the equilibrium between active and inactive receptor conformations, which has been noted for other AT_2R ligands.[101,102]

Aims

With the first AT_2R antagonist entering phase II clinical trials as a potential treatment for neuropathic pain, there is a renewed interest to evaluate new AT_2R antagonists and elucidate their biological response. To better understand the biological relevance of the building blocks that constitute the AT_2R antagonist **C38**, three chemical moieties were explored to identify compounds with better drug-like properties. With knowledge gained during the initial phases of this project the overall aim of this thesis became to broaden the structure-activity relationship of **C38**, and identify compounds with superior ADME properties and affinity for human AT_2R compared to **C38**.

The specific aims were to:

- Investigate microwave-heated continuous-flow as a method for quick generation of a compound library to investigate structure-activity relationships.
- Evaluate the importance of the sulfonyl carbamate chain in **C38** for both affinity to human AT_2R and metabolic/chemical stability.
- Investigate if the phenyl ring in the **C38** scaffold is a site of phase I metabolism and if this can possibly be counteracted while improving or retaining affinity for human AT_2R.
- Explore a bicyclic amide moiety as a possible replacement of the CYP-sensitive imidazole of **C38**.

In addition, the importance of knowing the functional activity of a ligand was apparent and thus, the following specific aim was included

- Identify and evaluate an assay to investigate the functional activity of AT_2R ligands.

Transesterification of Sulfonyl Carbamates and the Applicability of Microwave Heated Continuous-Flow (Paper I and II)

Background and Strategy

Sulfonyl carbamates exhibit very similar acidic properties to carboxylic acids[103,104], making them useful as bioisosteres. There are several hundred reported compounds containing the sulfonyl carbamate moiety with biological activity on targets within the renin-angiotensin-aldosterone system, including ligands for the Mas receptor, AT_2R, and AT_1R. A majority of the AT_2R ligands presented by our research group over the past two decades contain an alkyl-(arylsulfonyl)-carbamate function.[92,105] With the research group's long experience of sulfonyl carbamates, it was unexpected to find that the sulfonyl carbamate was susceptible to alkoxyl-alkoxy transesterification while storing an AT_2R ligand in methanol overnight (LC-MS sample). Searching the literature revealed no previous examples of such a reaction, although Hirama et al. reported an aryloxy-alkoxy transformation in 1984.[106] An early report noted that sulfonyl carbamates are stable under alkaline conditions, but can be slightly susceptible to hydrolysis at elevated temperatures in neutral aqueous solutions, as the acidic proton can act as an auto-catalyst.[104] In a previous project in our research group, the sulfonyl carbamate had been transformed into a sulfonylurea using a secondary alkyl amine.[95]

Using the discovered transesterification of sulfonyl carbamates with alcohols could allow the generation of a broad library of sulfonyl carbamate analogues to study the structure-activity relationship of a biologically interesting ligand, without requiring access to the respective alkyl chloroformates. Minimizing the use of chloroformates and replacing them with alcohols would serve as a safer, easier, and more cost effective alternative. Further, this transesterification could be performed in the microwave heated continuous-flow system available in our laboratory. Hence, convenient microwave batch conditions were established for the transesterification of sulfonyl carbamates using methyl tosylcarbamate as a model substrate. After this, the reaction was investigated in our microwave heated continuous-flow system, and the applicability of the latter protocol to biologically relevant compounds was determined.

Microwave Heated Continuous-Flow

Microwave heating is a well-established method for small-scale organic synthesis with numerous reaction protocols available. Microwave heating has been useful in the synthesis of biologically interesting compounds in many research labs and pharmaceutical companies.[107–109] Replacing conventional heating methods with devoted microwave heated laboratory instruments often improves heating rates and reduces reaction times. Pressurized reactions can be safely performed in the steel cavity of the microwave reactor, and both increased yield and selectivity have been observed.[107,110–114] Despite the great advantages of microwave heating, and the extensive use in early drug discovery programs, the physical restrictions associated with microwave heating limit the ability to scale up reactions. The penetration depth of microwaves is only a few centimeters in most reaction systems, and the dimensions of available standing wave cavities are limited.[110,115]

Combining microwave heating with a continuous-flow system could overcome the issue of scalability, while making the production safer and more efficient. Although continuous-flow processes are widely used in the petrochemical and bulk chemical industries, their use in the pharmaceutical industry and academia has been limited. In later years, the benefits associated with continuous-flow have increased the interest to use it to synthesize biologically interesting compounds, and a large number of varied organic syntheses have been successfully performed in continuous-flow.[116–119] The most common heating method in continuous-flow is conventional heating and replacing this with microwave heating adds advantages in safety and handling.[120–128]

The purpose-built continuous-flow system available in our laboratory uses non-resonant microwave heating (Figure 5). This allows high process temperatures, fast adjustment of reaction temperature, as well as improved safety.[126,129–131] In our setup, the reaction mixture is pumped through a 200×2 mm microwave transparent borosilicate tube reactor using an HPLC pump. Exposing the reaction mixture to a uniformly distributed axial microwave field allow homogenous heating. Fitting the system with a 1.0 mL injection loop minimizes the waste of expensive reagents and intermediates; an important element in medicinal chemistry programs. The short process time in the system, facilitates quick optimization of reaction parameters, e.g. solvent, temperature, reagent concentration, or molar ratio of reactants.

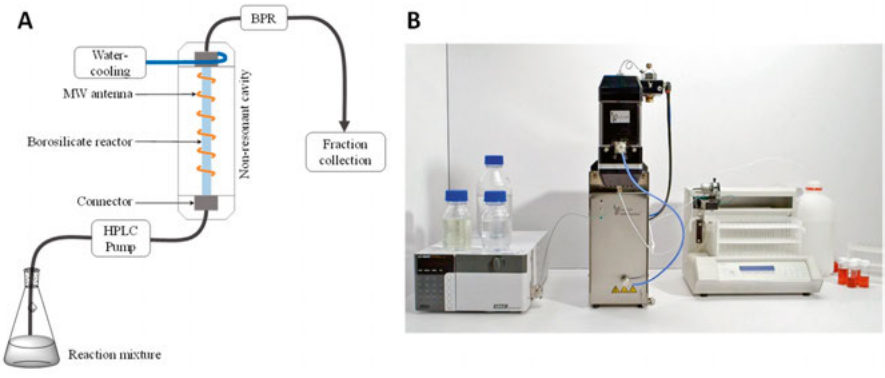

Figure 5. **A**) Schematic view of the microwave heated continuous-flow system. The HPLC pumps the reaction mixture through the system. In the non-resonant reaction cavity, the microwave (MW) antenna winds around the 200×2 mm borosilicate reactor heating the reaction mixture. A backpressure regulator (BPR) ensures a stable pressure profile in the system. After cooling, the reaction mixture can be collected in fractions or in batches. **B**) Photograph of the microwave heated continuous-flow system.

Reaction Scope in Batch Mode

Transesterification of sulfonyl carbamates at room temperature is slow, and to decrease reaction time we performed a temperature scan in a microwave heated batch system. Leaving a solution of the model substrate, methyl tosylcarbamate, in alcohol at room temperature will result in only a few percent conversion after 24 h. To decrease the reaction time, a solution of methyl tosylcarbamate **1** in *n*-butanol (0.1 M) was microwave heated in a septum-sealed vial for 20 min at various temperatures (Table 1). Analyzing the reaction mixtures with LC-UV/MS revealed three compounds (**1**, **2a**, and **3**). Assuming the compounds have similar UV response, the UV 254 nm peak area percent of each detected component was compared. This revealed low conversion to butyl carbamate product **2a** when heating the mixture at 60 °C. Increasing the temperature to 80 °C improved conversion, but 50% of the methyl tosylcarbamate **1** remained. At 100 °C the major component on LC-UV/MS was the butyl carbamate product **2a**, isolated in 88% yield. At this temperature, only small amounts of the starting material **1** and the by-product, primary sulfonamide **3**, were detectable. Further increasing the temperature to 120 °C did not improve the product yield (90%), but no starting material was detectable at this temperature. As the undesired by-product **3** increased at higher temperatures, the optimal temperature range under these conditions was determined to be 100-120 °C.

The reaction mechanism probably follows an acid catalyzed Fisher-type transesterification pathway. Heating methyl tosylcarbamate in a solution of

n-butanol, acetonitrile and water (2:1:1) generated only primary sulfonamide **3**. In addition, no intermediate sulfonyl isocyanate was detected in any of the reaction mixtures. These results in combination with the reported self-catalyzing property of the sulfonyl carbamate *N*-proton[104], support by-product **3** forms following hydrolysis and subsequent decomposition to the primary sulfonamide.

Table 1. *Optimizing temperature for the transesterification of sulfonyl carbamates.*

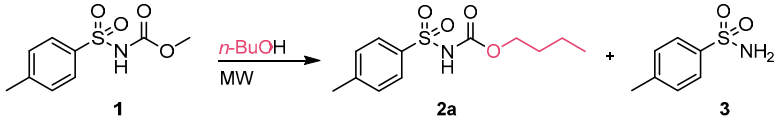

1 **2a** **3**

Entry	T [°C]	Area (%) **1**[a]	Area (%) **2a**[a]	Area (%) **3**[a]	Yield **2a** (%)[b]
1	60	93	7	ND[c]	-
2	80	53	45	ND[c]	-
3	100	4	94	2	88
4	120	ND[c]	95	5	90
5	140	ND[c]	89	11	-

Reaction mixture (0.1 M), MW-heated at the indicated temperature for 20 min. [a] Results reported as peak area percent at UV 254 nm chromatogram using LC-UV/MS. [b] Isolated yield after purification using silica gel column chromatography. [c] ND = Not detectable.

Successful transesterification of the model substrate **1** with various primary, secondary, and tertiary alcohols, generated a small library of new sulfonyl carbamates (Figure 6). The optimal reaction conditions in microwave heating had been set to 120 °C for 20 min based on the temperature scan. However, it quickly became apparent that these conditions were not optimal for all tested alcohols, resulting in formation of primary sulfonamide **3** and other decomposition products. The reaction temperature was set to 100 °C for 20 min for aliphatic isopentyl **2b** and cyclopentane **2c**, generating both products in good yields. For chlorobutyl **2d,** terminal alkyne **2e**, benzyl **2f**, and *tert*-butyl **2g** the initial reaction conditions of heating at 120 °C for 20 min worked well and resulted in moderate to good yield of the desired products. Heating the reaction mixture for 30 min at 100 °C gave terminal allyl **2h** in good yields. Applying the same conditions to obtain chloroethoxy-ethyl **2i** gave only a slight improvement in yield as compared to the standard conditions (64% cf. 57%). Terminal alkyne **2j** displays a similar trend; heating the reaction for 60 min at 100 °C resulted in the same yield as when the reaction was performed under standard conditions.

As the initial optimization had been established for *n*-butanol, other methyl (aryl)-sulfonyl carbamates were successfully investigated in *n*-butanol (Figure 6). A strongly electron donating group (methoxy **2k**), and both weakly and strongly electron withdrawing groups (bromo **2l** and trifluoromethoxy **2m**) gave good yields under the standard conditions. Reducing the reaction temperature to 100 °C produced nitro compound **2n** in moderate yield.

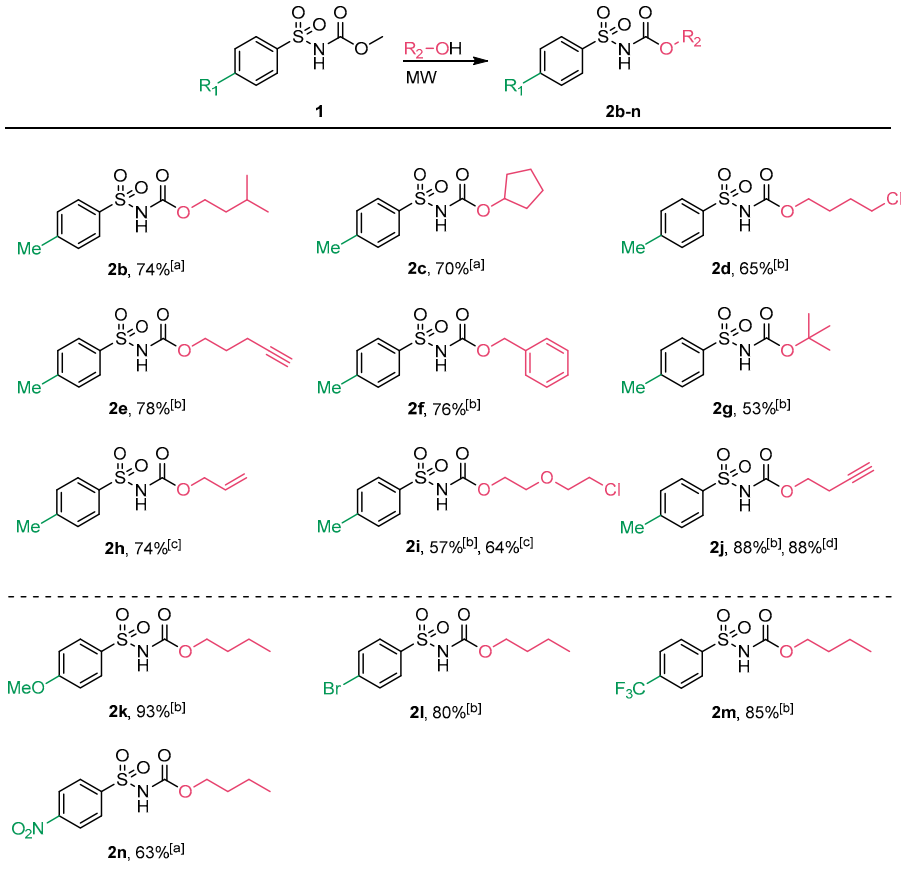

Figure 6. Reaction scope for transesterification of sulfonyl carbamates under batch conditions (0.1 M solutions). Isolated yields after purification using silica gel column chromatography (>95% pure by ^{1}H NMR). [a] MW-heating for 20 min at 100 °C. [b] MW-heating for 20 min at 120 °C. [c] MW-heating for 30 min at 100 °C. [d] MW-heating for 60 min at 100 °C.

Reaction Scope in a Continuous-Flow System

Evaluating the model reaction in the microwave heated continuous-flow system revealed that higher temperatures were necessary to obtain the products in good yields at a 1 min/mL flow rate (Table 2). Heating a solution of methyl tosylcarbamate (0.04 M) in neat *n*-butanol at 120 °C and with a flow rate of 1.0 mL/min, gave only 33% yield when analyzing the product mixture with LC-UV/MS. This is probably due to the short residence time (38 s). Increasing the temperature to 160 °C or 180 °C achieved full conversion and generated butyl carbamate **2a** in 98% and 95% yield respectively, without observing decomposition or formation of primary sulfonamide. However,

heating the reaction mixture above 180 °C resulted in reduced yields due to an unidentified decomposition.

The short process time in the system allowed quick optimization for all alcohols tested in neat conditions, generating high product yields for all tested alcohols (Table 2). The microwave heated continuous-flow system reached stable temperatures after less than 30 s with the tested reactants. Thus, the washout period (3 min) became the limiting factor in the system making quick optimization possible. Notably, the isobutyl **2o** analogue was isolated in a lower yield than *sec*-butyl **2p**, 75% and 97% respectively, at the optimal temperature 160 °C, due to decomposition. Propyl **2q** and isopropyl **2r** did not display the same trend, and both were isolated in excellent yields at all tested temperatures. Pentyl **2s** and butenyl **2t** decomposed slightly at the highest temperature (200 °C) tested, but both were isolated in good yields at 160 °C. The benzylic compound **2f** and tertiary amine **2u** were isolated in good yields at 180 °C. Cyclopropyl methyl **2v** was isolated in 93% yield at 160 °C; but increasing the temperature further only resulted in decomposition of the product.

To explore the robustness and scalability, the model reaction was scaled out using a more concentrated reaction mixture to further increase output. Heating methyl tosylcarbamate in *n*-butanol (0.1 M) at 180 °C and at a flow rate of 1.0 mL/min (38 s res. time) for 45 min, generated 1.1 g (91%) of butyl carbamate **2a**. The increased concentration of the reaction mixture did not limit the yield or decrease the quality of the product mixture, enabling a productivity of 5.4 mmol/h to be obtained in our system.

Making use of a co-solvent could help minimize waste of expensive reactants, and increase the scope of the reaction by increasing solubility. Acetonitrile presented as a good co-solvent due to high reagent solubility, easy handling, and low cost. The low boiling point of the solvent is associated with high pressure, but an initial quick solvent scan in the microwave heated continuous-flow system revealed high temperatures could be reached for acetonitrile and no decomposition was noted. The model reaction was initially prepared as a 0.2 M solution with 12 mol equivalents of *n*-butanol. The isolated yields at 160-180 °C were moderate (47-49%, data not shown in Table 2) at the flow rate 1.0 mL/min (38 s res. time). Elevating temperatures to 180-200 °C and reducing flow rate to 0.5 mL/min (76 s res. time) improved the yields to 71-74% (data not shown in Table 2). Increasing the temperature further was not possible due to the generation of high pressure and thus, the excess of *n*-butanol was increased to 28 mol equivalents. This generated butyl carbamate **2a** in slightly increased yield (80-81%) at 200-220 °C. Because of the pressure limitations in the system, the maximum yield when using acetonitrile as co-solvent remained slightly lower compared to the neat system. However, this was not true for all tested alcohols; iso- and *tert*-butanol (28 equiv.) were reacted with methyl tosylcarbamate dissolved in acetonitrile

(0.2 M solution), generating **2o** and **2g** in similar yields as in the neat system (63% and 53%).

Fitting the system with an injection loop saved expensive material while maintaining yields. Although the co-solvent system worked well, the high concentration of reagents did not save reagents to the extent needed in a medicinal chemistry program. Hence, a stock solution of methyl tosylcarbamate in acetonitrile (0.2 M) was prepared, with 29-49 mol equivalents of the alcohol (Table 2). Injecting the solution into a carrier flow of acetonitrile (1.0 mL/min, 38 s res. time) at 160 °C, gave **2a** in 67% yield. Changing the flow to 0.5 mL/min (76 s res. time) did not improve yields, and thus the reaction temperature had to be increased. At 200 °C and 220 °C the yields of **2a** were good (81% and 72%) but still slightly reduced in comparison to the neat conditions. Isobutyl **2o**, *sec*-butyl **2p**, isopropyl **2r**, and pentyl **2s** were all isolated in similar yield using the loop injection as in the neat system, while the yield reduced slightly for propyl **2q** and allyl **2t**.

No measurements of the concentration profile were conducted, but we hypothesize that the injection plug suffer from some tailing which may cause the slight decrease in yield. The axial dispersion and the back mixing caused by the laminar flow, in addition to the junction turbulence, will likely cause some dispersion of the injection plug.

Table 2. *Transesterification in the microwave heated continuous-flow system.*

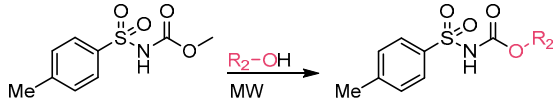

1 **2a, 2f-g, 2o-v**

Cmpd	R_2	T [°C]	Yield [%] neat[a]	Yield [%] MeCN[b]
2a		140	66	-
		160	98[c]	67[d], 63[e]
		180	95, 91[f]	85[d], 80[e]
		190-195	-	78[g]
		200	88	80, 81[d]
		210	96[c]	-
		220	-	81, 72[d]
2o		160	75	-
		180	67	68[d]
		200	43	53[d]
		220	-	63
2p		160	97[c]	-
		180	97[c]	82[d]
		200	86	76[d]
2q		160	96[c]	-
		180	97[c]	84[d]
		200	96[c]	76[d]
2r		160	88	-
		180	83	85[d]
		200	89	68[d]
2s		160	88	-
		180	87	80[d]
		200	75	69[d]
2t		140	59	-
		160	91	-
		180	89	62[d]
		200	55	-
2f	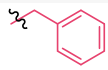	180	74	-
		200	74	-
2u	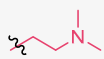	160	74	-
		180	80	-
		200	72	-
2v		160	93	-
		180	85	-
		200	76	-
2g		220	-	53

Yields of isolated products generated using MW-heating in the 200×2 mm borosilicate reactor, and purified by silica gel column chromatography (>95% pure by ^{1}H NMR). [a] A 0.04 M solution of **1** in neat alcohol, flow rate 1.0 mL/min (38 s res. time). [b] A 0.2 M solution of **1** and 28 equiv. alcohol in MeCN, flow rate 0.5 mL/min (76 s res. time). [c] No column chromatography. [d] A 0.2 M solution of **1** and 29-49 equiv. alcohol in MeCN, 1.0 mL injection in MeCN flow at rate 1 mL/min (38 s res. time). [e] 1.0 mL injection, flow rate 0.5 mL/min (76 s res. time). [f] Scale out, a 0.1 M solution of **1** and *n*-butanol, flow rate 1.0 mL/min (38 s res. time), 45 min collection. [g] 1.0 mL injection, flow rate 1.5 mL/min (19 s res. time).

Application to Biologically Relevant Compounds

The use of the microwave heated continuous-flow system to generate biologically interesting compounds was demonstrated using the AT_2R agonist **C21** to form three previously published[95] AT_2R ligands (Table 3). A solution of **C21** dissolved in neat alcohol (0.2 M) was injected via the loop, with the carrier solvent being the same alcohol. Without optimizing the temperature, all reactions with **C21** proceeded well, with fair yields (41-64%) at 180 °C. The reactions did not reach full conversion and separation of **C21** and **4a-c** on preparative HPLC was poor, reducing the yields. Optimizing the reaction would likely have resulted in complete conversion and increased yields, although the dispersion of the injection plug could still result in some loss of material. For comparison, generating compound **4c** in the microwave-batch system resulted in complete conversion and significantly increased the yield to 82%.

Table 3. *Transesterification of AT_2R agonist **C21**.*

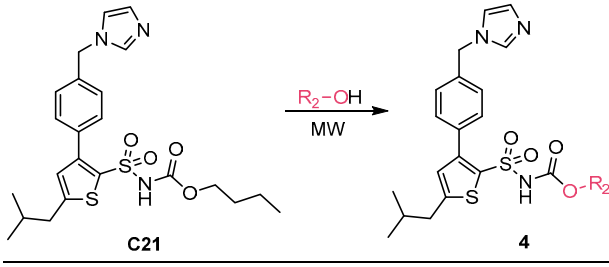

Cmpd	R_2	Yield [%][a]	Yield [%][b]	AT_2R K_i [nM][c]	AT_1R K_i [nM][c]
4a		41	-	37	> 10 000
4b		51	-	75	> 10 000
4c		64	82	10	> 10 000

Yields of isolated products generated using MW-heating in the 200×2 mm borosilicate reactor, and purified by preparative reverse-phase HPLC (>95% pure by ^{1}H NMR). [a] A 0.2 M solution of **C21** in neat alcohol was injected in a flow of the same alcohol at rate 1 mL/min (38 s res. time), and heated at 180 °C. [b] Batch MW-heating of **C21** in ethanol for 20 min at 120 °C. [c] For biological data see reference 95.

Summary and Future Outlook

Transesterification of sulfonyl carbamates is a simple and quick reaction with a broad scope and applicability in both microwave batch and continuous-flow system. Using transesterification of sulfonyl carbamates with alcohols, instead of reacting sulfonamides with various alkyl chloroformates, presents a cost effective and safe alternative for expanding the structure-activity relationship of biologically active compounds. Quick optimization of the reaction conditions in each system generated a range of tosylcarbamates in good to high yields. In the microwave heated continuous-flow system, reactions could be safely run at significantly higher temperatures than the batch system, without detecting the primary sulfonamide by-product or decomposition. The short processing time and the possibility to run reactions at high temperatures while maintaining safety are the key features of the microwave heated continuous-flow system. Using an injection loop and acetonitrile as a carrier solvent reduced use of materials and increased solubility, with only slight reduction in yield compared to the neat system. The injection loop was useful when generating three known AT_2R ligands from the selective AT_2R agonist **C21**. The yield was better in the batch system, as no material was wasted. Thus, using the transesterification in the batch system is likely better for late stage functionalization. The short reaction time, facilitating quick optimization, in the continuous-flow system will be more useful for compounds with fewer reaction steps.

Structure-Activity Investigation of **C38**, a Reported AT_2R Antagonist (Papers III and IV)

Background

Evaluating the affinity to human AT_2R of agonist **C21** and antagonist **C38** revealed retained affinity for **C21** compared to pig AT_2R, while the affinity for **C38** was significantly reduced (19 nM vs 270 nM, Figure 7**A**). The AT_2R ligands developed by our research group during previous years were evaluated in a displacement assay employing membrane preparations from pig uterus myometrium. This assay was no longer available in house and thus, a new assay was identified for the compounds evaluated in this thesis. The new assay uses displacement of the radioligand [^{125}I][Sar^1,Ile^8]-angiotensin II from human AT_2R expressed in HEK-293 cells (membrane preparations). Re-evaluating five known AT_2R ligands in the new human AT_2R assay revealed that the agonist **C21** exhibited similar affinity to human AT_2R as it had shown towards pig AT_2R, and the amides **C93** and **C97** also retained affinity (Figure 7**A**). The same was not true for antagonist **C38**, exhibiting a 14-fold reduction in affinity. Ligand **C102**, having previously exhibited a very high affinity for pig AT_2R, displayed a 190-fold reduction in affinity when tested against human AT_2R.

In a 2014 report, Behrends et al. discussed the affinity difference between pig and human AT_2R for peptidomimetic ligands.[132] They noted a significant drop in affinity for the peptidomimetic compounds, comparable to the reduced affinity seen for **C38** and **C102**. Behrends et al. hypothesized the different tissues used in the two assays (endogenous membranes versus transfected kidney cells) could be the cause of the reduced affinity. Species difference may also be the cause however, the amino acid sequence is highly conserved between pig and human AT_2R (95% sequence identity)[133–135]. Functional diversity due to species difference is rare for highly conserved proteins and in addition, the endogenous ligand AngII, compounds **C21**, **C93**, and **C97** all display comparable results in both assays (Figure 7**A**). Investigating why the affinity varies for ligands between the two assays is beyond the scope of this thesis, but could be important for future work. If the cause is due to the variations between species, this could greatly affect moving forward with potential drug candidates in pre-clinical studies involving animals. Moving

forward with lead candidates would then require ensuring, and probably optimizing, affinity towards several species.

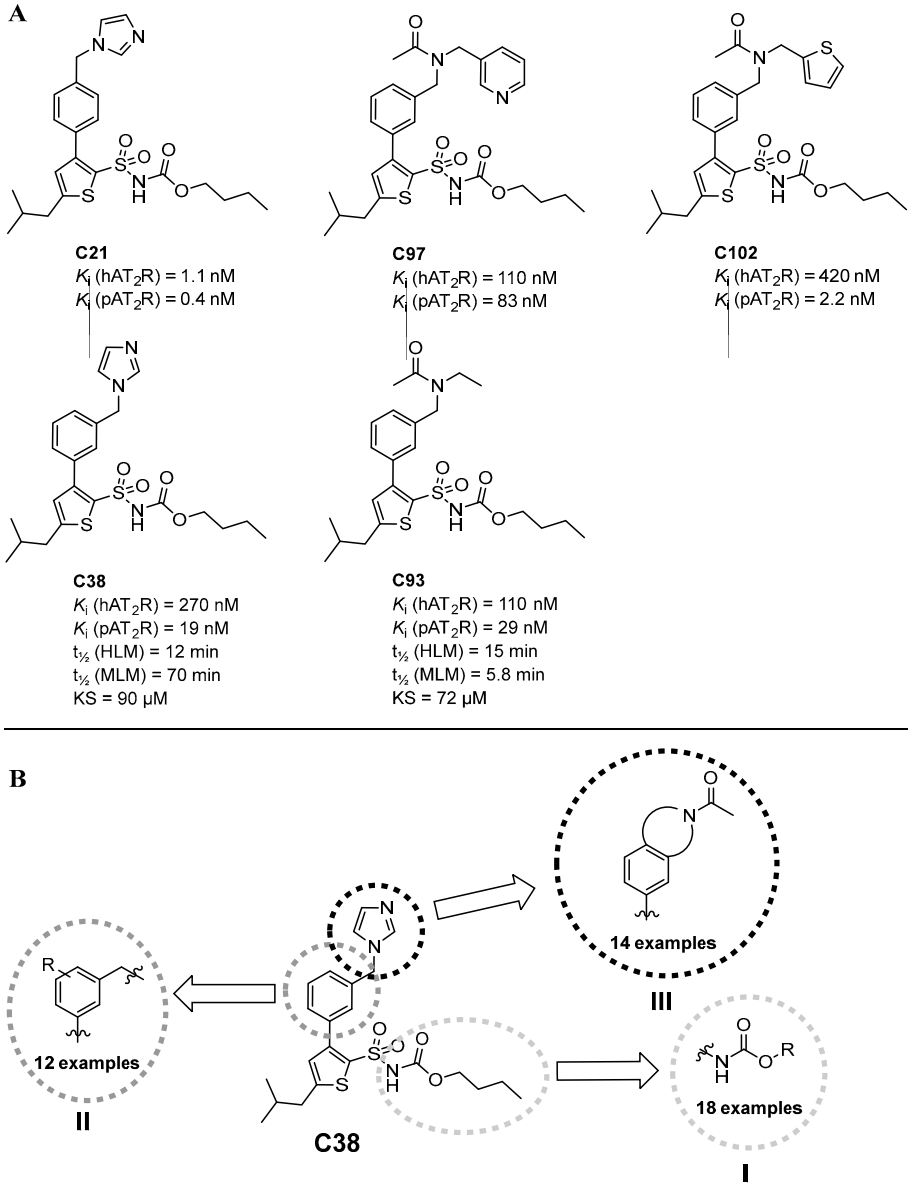

Figure 7. **A**) Known AT$_2$R ligands. Affinity for AT$_2$R (K_i), metabolic stability in human liver microsomes (HLM), mouse liver microsomes (MLM), and kinetic solubility (KS) **B**) The three motifs explored in this thesis: the sulfonyl carbamate (I), the phenyl ring (II), and the bicyclic amide replacing the imidazole (III).

When evaluating the in vitro metabolic stability of **C38** and **C93** using human and mouse liver microsomes, neither compound exhibited good stability (Figure 7**A**). This indicates that both compounds will likely display high in vivo clearance, which will impact the biological exposure. While the half-life of **C38** was fair in mouse microsomes (70 min), the half-life in human microsomes was only moderate (12 min). The amide **C93** had unsurprisingly poor stability in mouse liver microsomes (5.8 min), and exhibited similar stability as **C38** in human microsomes (15 min). The kinetic solubility was acceptable for both compounds. The purpose of the structure-activity studies of **C38** presented in this thesis was to improve affinity towards human and metabolic stability in mouse/human liver microsomes, while retaining or improving the kinetic solubility. My work focused on exploring three chemical moieties: the sulfonyl carbamate, the phenyl ring, and the imidazole ring (Figure 7**B**).

Synthesis and Evaluation of Sulfonyl Carbamate Analogues (Paper III)

Strategy

The previous studies of the **C38** scaffold has not explored the sulfonyl carbamate moiety[69,100] as the agonist project had found this site to be highly sensitive to changes. In 2006, Wu et al. explored the sulfonyl carbamate chain of the **C21** scaffold using the pig uterus myometrium assay.[95] Synthesizing a small library of 12 compounds revealed few modifications were possible in this position without observing significantly reduced affinity (25- to 190-fold reductions). The study revolved only around the agonistic **C21** scaffold and was not applied to the antagonistic **C38** structure. Combined with the newly discovered reduced affinity of **C38** in the human AT_2R affinity assay, exploring the sulfonyl carbamate for the **C38** scaffold was warranted.

Using the transesterification presented in the previously chapter of this thesis, a series of varied sulfonyl carbamate chain were synthesized. In addition, acyl sulfonamides and sulfonylureas were evaluated as possible replacements for the sulfonyl carbamate. The new ligands were evaluated for affinity towards human AT_2R and metabolic stability in both human and mouse liver microsomes.

Synthetic Work

Modifying the synthetic pathway previously used in our research group simplified the reaction and generated the key building block, the MIDA protected boronic acid (Figure 8). Microwave assisted Negishi coupling of 5-bromo-*N*-(*tert*-butyl)thiophene-2-sulfonamide **5** with isobutylzinc bromide

replaced the lithiation/alkylation protocol previously used[63,136] to generate *N*-(*tert*-butyl)-5-isobutylthiophene-2-sulfonamide **6**. This reduced the purification time as the lithiation/alkylation protocol is difficult to control and usually results in over-alkylated by-products. The thiophene boronic acid **7** was obtained after lithiation/borylation of thiophene **6**. The syrup-like boronic acid **7** is difficult to handle and thus, was converted to the MIDA boronate **8**, which is solid and stable at ambient temperature.[137]

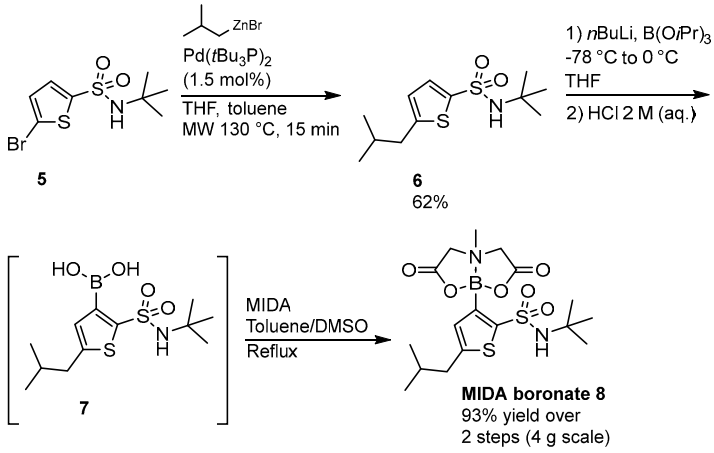

Figure 8. Synthesis of key intermediate, the MIDA boronate **8**.

Direct alkylation of imidazole with 3-bromobenzyl bromide **9** generated 1-(3-bromobenzyl)-1*H*-imidazole **10** (Figure 9). Coupling this intermediate with MIDA boronate **8** under Suzuki conditions produced thiophene-benzyl-imidazole **11** in high yield.

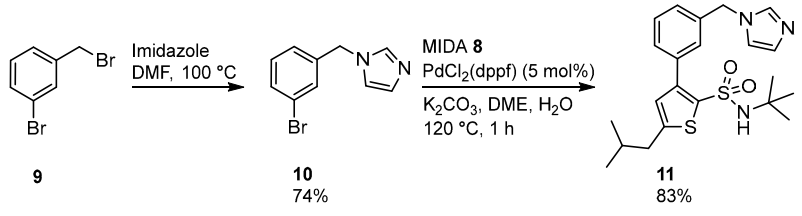

Figure 9. Alkylation generated the 3-bromobenzyl imidazole **10**. Suzuki coupling with MIDA boronate **8** produced thiophene-benzylimidazole **11**.

Treating the *tert*-butyl sulfonamide **11** with trifluoroacetic acid generated the primary sulfonamide **12** in good yield (Figure 10). This was subsequently coupled with butyl chloroformate to give **C38** in good yield.

AT_2R ligand **C38** was reacted with various alkyl alcohols under batch transesterification conditions using microwave batch heating, generating 11 products in fair to good yield (26-85%) (Figure 11). As 2-methoxyethanol requires a special permit for use and handling, the 2-methyxoethyl **13c** was

synthesized by coupling primary sulfonamide **12** with 2-methoxyethyl chloroformate. When exploring the scope of the transesterification of sulfonyl carbamates, the sterically hindered *tert*-butanol could be successfully reacted with methyl tosylcarbamate. When attempting the reaction with **C38** only primary sulfonamide **12** was isolated, which might be due to the bulk of both substrates. The *tert*-butyl sulfonyl carbamate **13k** was instead generated in good yield (80%) by reacting primary sulfonamide **12** with Boc anhydride.

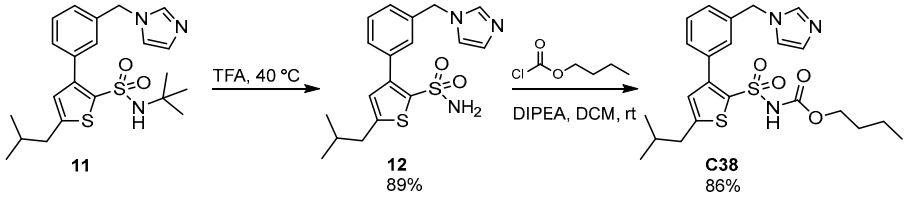

Figure 10. Deprotection generated primary sulfonamide **12**. Reacting **12** with butyl chloroformate generated the reported antagonist **C38** in good yield.

Microwave assisted aminolysis of **C38** with primary or secondary alkylamines allowed for the formation of sulfonylureas **13g** and **13q** (Figure 11). Reacting primary sulfonamide **12** with either acid chlorides or anhydrides generated the acyl-sulfonamides **13f**, **13o**, and **13p**.

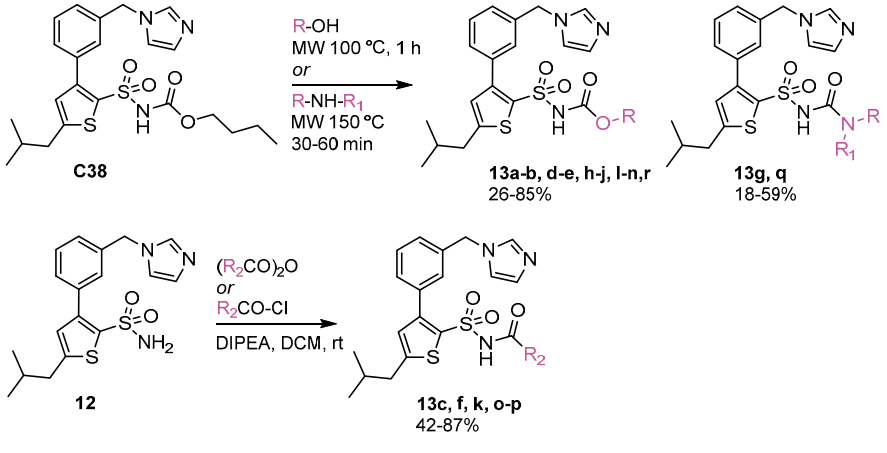

Figure 11. Transesterification and aminolysis of **C38** successfully generated 13 new AT_2R ligands. Reacting primary sulfonamide **12** with chloroformate, acid chlorides or anhydrides generated an additional 5 new AT_2R ligands.

Results and Discussion

Investigating the affinity of the new AT_2R ligands revealed a flat structure-activity relationship, a majority of the ligands being equipotent to **C38** (Figure 12**A-C**). All tested ligands retained selectivity to human AT_2R over human AT_1R (data not shown). Focusing initially on the sulfonyl carbamates showed that branching, shortening, and extending the alkyl carbamate chain did not affect affinity to human AT_2R, in contrast with previous knowledge relating to the **C21** scaffold. In addition, the trifluoromethyl **13r** was surprisingly active on AT_2R, though 3-fold reduced compared to **C38** (Figure 12**D**). In 2006, Wu et al. generated a ligand of the **C21** scaffold using the same chain, which exhibited no measurable affinity towards pig AT_2R.[95] While the assays used differ and do not produce fully comparable results, it is interesting to note that a higher variability is allowed around the sulfonyl carbamate moiety in the human AT_2R assay as compared to the pig AT_2R assay.

Investigating the in vitro metabolic stability in human and mouse liver microsomes revealed that size and lipophilicity of the side-chain are important factors. Reducing the lipophilic chain clearly and perhaps not surprisingly increased the metabolic stability. In general, the compounds in this first series are less prone to undergo phase I metabolism in mouse liver microsomes compared to human liver microsomes. The notable exception is *sec*-butyl **13h**, exhibiting a fair and similar stability in both assays (HLM = 43 min cf. MLM = 47 min). The best ligands generated were methyl **13a** and ethyl **13b** (Figure 12**A**). Both ligands are equipotent with **C38**, and exhibit good metabolic stability in both human and mouse liver microsomes. This indicates exposure after administration in an in vivo model will likely be good, making them both promising for future work in murine models of neuropathic pain.

Replacing the sulfonyl carbamate with sulfonylurea did not yield any improvement in affinity or metabolic stability. Butyl urea **13g** displayed similar properties as **C38**, with comparable affinity and metabolic stability in both human and mouse liver microsomes (Figure 12**B**). A 10-fold reduction in affinity was noted for diethyl urea **13q** and hence, not warranting an investigation of the metabolic stability (Figure 12**D**). Of the three synthesized acyl sulfonamides, neither exhibited improved properties compared to **C38**. While cyclopropane **13f** was comparable to **C38** in both affinity and metabolic stability, ethyl **13o** and butyl **13p** were inferior due to low metabolic stability (Figure 12**B-C**).

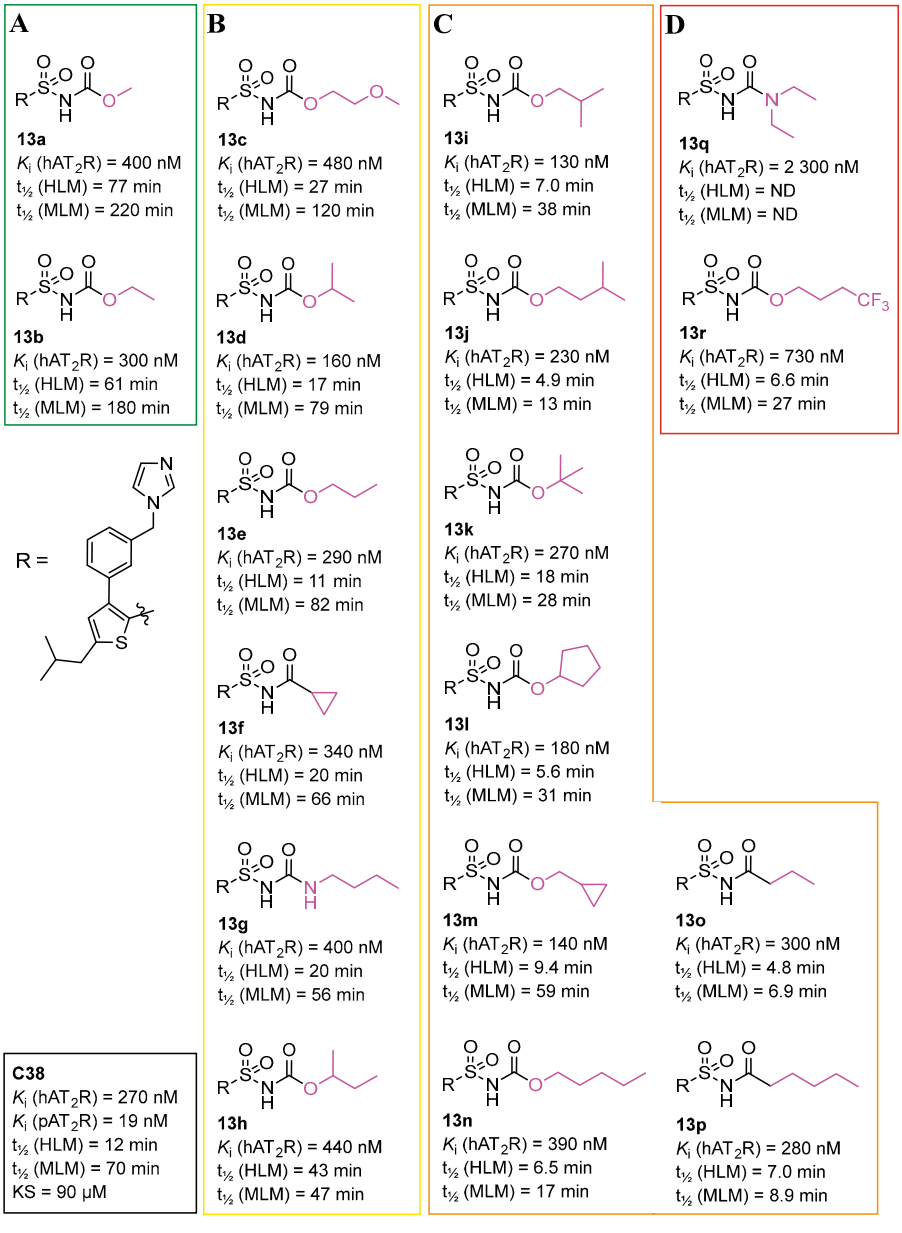

Figure 12. Summary of the AT_2R ligands generated to explore the sulfonyl carbamate moiety of **C38**. The affinity for human AT_2R (K_i), and the metabolic stability in human liver microsomes (HLM) and mouse liver microsomes (MLM) was determined. **A**) Two compounds exhibited improved metabolic stability in mouse and human microsomes, while retaining affinity. **B**) Six ligands showed retained affinity and metabolic stability. **C**) Eight compounds displayed similar affinity as **C38**, but exhibited reduced metabolic stability. **D**) Two ligands were inferior to **C38** regarding both affinity and metabolic stability.

Synthesis and Evaluation of Phenyl-Ring Derivatives (Paper IV)

Strategy

During previous endeavors, the phenyl ring of the **C38** and **C21** scaffolds has been sparsely explored, as early studies indicated the site was sensitive to changes. In 2004, Wan et al. concluded that the thiophene and the phenyl ring must be bound to each other directly without an intermediate methylene on the **C21** scaffold, as adding a methylene renders the ligands inactive.[63] Further work presented by Murugaiah et al. in 2007, showed that for the **C21** scaffold, replacing the phenyl ring with a pyridine or thiophene gave inactive compounds. However, replacing the phenyl with a furan was allowed but resulted in a 20-fold reduction of affinity towards pig AT_2R.[96]

The structure-activity relationship of the phenyl ring has never been investigated for the **C38** scaffold, and addition of small substituent to it has not been explored previously for either scaffold. The phenyl ring could be a site of phase I oxidation and with the hope of improving the metabolic stability, adding small substituents to the phenyl ring of the **C38** scaffold was explored. Despite data from Murugaiah et al. in 2007 indicating the pyridine was not suitable for the **C21** scaffold, three ligands with pyridine instead of phenyl were synthesized in order to investigate if this could help improve solubility of the compounds.

Synthetic Work

To obtain the substituted benzyl- and pyridine-analogues, the synthetic pathway outlined in the previous section was used (Figure 8-10). Direct alkylation of 3-halo benzylbromides (**14a**, **14c**), or chlorination/mesylation of the 3-bromo benzylalcohols (**14b**, **14d--l**) followed by imidazole alkylation, generated the substituted benzylimidazoles (**15a-r**, **15i-l**) and pyridine-methylene imidazoles (**15f-h**), Figure 13. The compounds were coupled with MIDA boronate **8** under Suzuki conditions, as described in Figure 9. Deprotecting the *tert*-butyl sulfonamides, and subsequently reacting the obtained primary sulfonamides with butyl chloroformate generated the products **16a-l** in low to fair yields over three steps (Figure 13). The low yields of product **16a**, **16i**, **16j**, and **16l** (3%, 3%, 4%, and 5% respectively) may relate to electronic and/or steric properties reducing the efficiency of the Suzuki coupling.

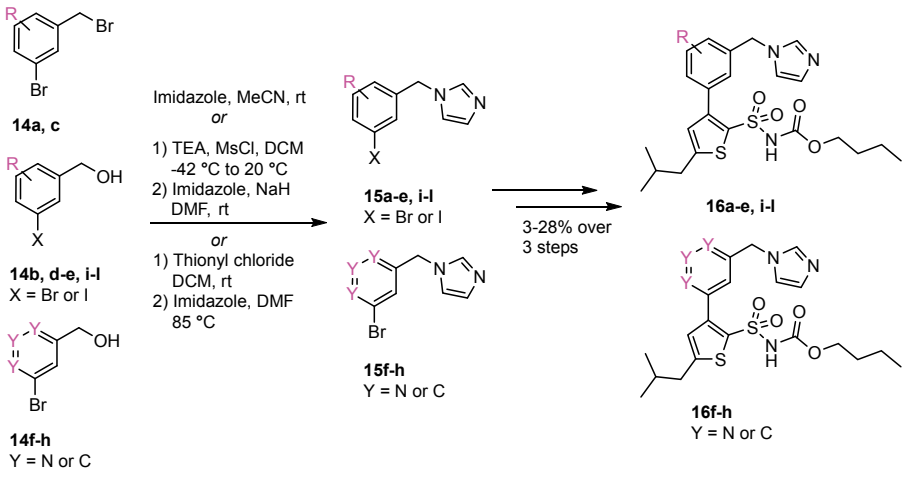

Figure 13. Synthesis of substituted benzyl- and pyridine-analogues. Direct alkylation, or chlorination/mesylation followed by alkylation, generated the substituted benzylimidazoles and pyridine-methylene imidazoles (**15a-l**). Subsequently, following the established synthetic pathway generated 12 new AT_2R ligands (**16a-l**).

Results and Discussion

Adding substituents to the phenyl ring or replacing it with a pyridine revealed substituents para to the thiophene retained affinity, while substituents ortho to the thiophene were less favorable (Figure 14**A-D**). Ligand selectivity for human AT_2R over human AT_1R was retained for all tested compounds (data not shown). Seven compounds retained affinity for human AT_2R compared to **C38**, and in four of these, the substituent was added to the para position relative to the thiophene: fluoro **16a**, trifluoromethoxy **16b**, bromo **16d**, and methyl **16e** (Figure 14**A-B**). A methoxy in the same position (**16l**) decreased affinity 5-fold (Figure 14**D**). This could relate to the lowered lipophilicity of the methoxy (**16l**) compared to the trifluoromethoxy moiety (**16b**), or possibly to the electron-donating properties of the substituent. Introducing a fluoro (**16i**) or methyl (**16j**) substituent in the ortho position relative to the thiophene resulted in a 3-fold reduction of affinity, which may relate to altered electronic properties or perhaps a steric interaction (Figure 14**D**). When adding a methyl substituent in the meta position (**16k**) a similar reduction was observed, however this was not seen for meta-fluoro **16c**. Replacing the phenyl ring with a pyridine ring furnished active compounds, in contrast to previous data.[96] The meta and ortho pyridine analogues (**16g**, **16g**) were equipotent to **C38**, while the para pyridine analog **16h** exhibited a slightly reduced affinity.

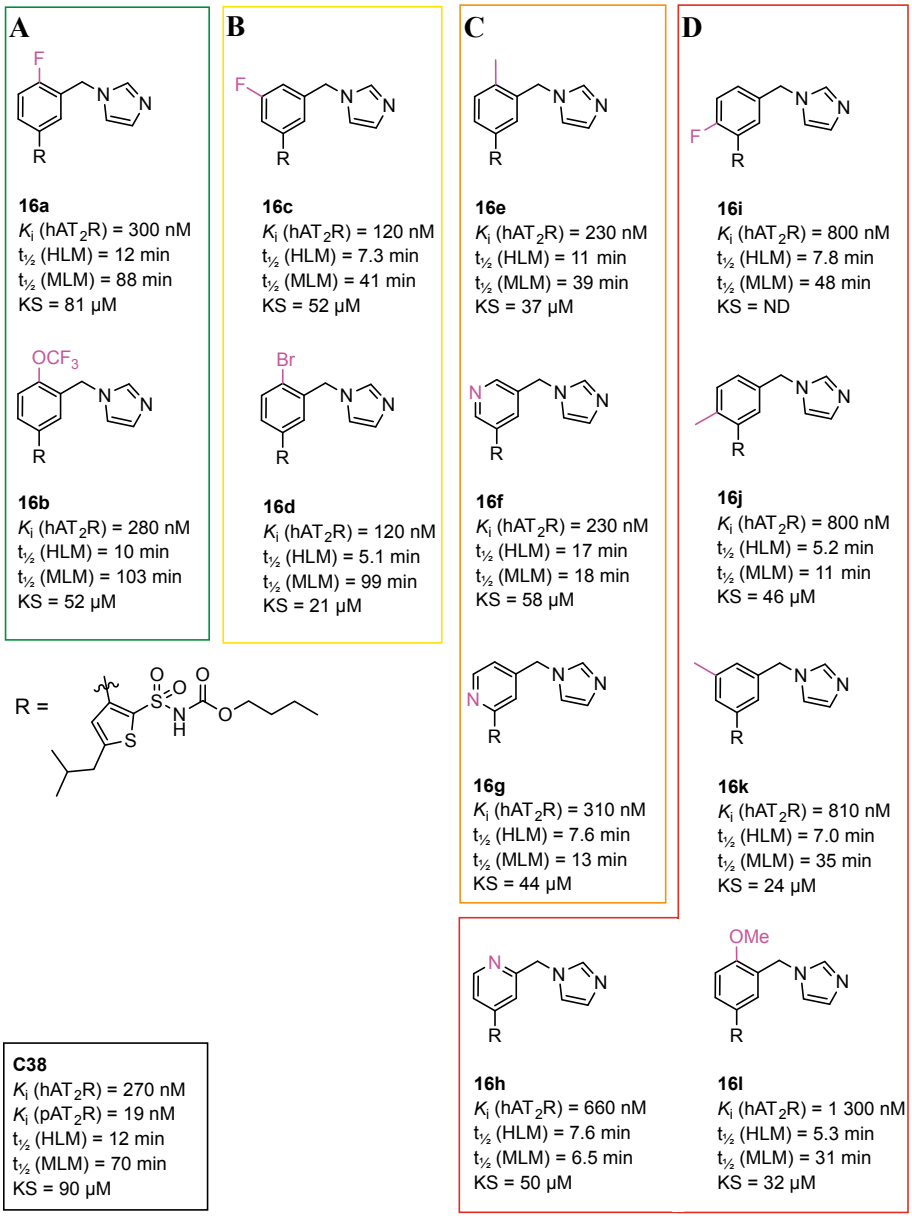

Figure 14. Summary of the AT_2R ligands generated to explore the phenyl ring of **C38**. The affinity for human AT_2R (K_i), the metabolic stability in human liver microsomes (HLM) and mouse liver microsomes (MLM), and the kinetic solubility (KS) was determined. **A**) Two compounds exhibited retained affinity, metabolic stability in mouse and human microsomes, and kinetic solubility. **B**) Two ligands showed retained affinity but the metabolic stability was reduced for **16c** and the kinetic solubility was reduced for **16d**. **C**) Three compounds displayed similar affinity as **C38**, but exhibited reduced metabolic stability. **D**) Five ligands were inferior to **C38** in regards to affinity, metabolic stability, and kinetic solubility.

Metabolic stability in human and mouse liver microsomes was not improved by adding substituents to the phenyl ring (Figure 14**A-D**). As noted for the sulfonyl carbamates, the ligands in this series were more prone to undergo metabolism in human liver microsomes than mouse microsomes. Introduction of a fluoro atom onto phenyl rings is a well-known strategy in medicinal chemistry to block phase I oxidation.[138,139] While affinity was retained when adding a fluoro atom in the para or meta position (**16a**, **16c**), the metabolic stability was not improved in human or mouse liver microsomes for any of the fluorinated compounds (**16a**, **16c**, and **16i**). Hence, the phenyl ring is likely not the main site for oxidative metabolism. Unsurprisingly, methylating the phenyl ring reduced metabolic stability as these lipophilic ligands are prone to undergo benzylic oxidation. The para-bromo **16d** exhibited a retained stability in mouse microsomes, while the stability of para-methoxy **16l** in both human and mouse liver microsomes was reduced.

Kinetic solubility was not improved by replacing the phenyl ring with a pyridine ring (Figure 14**C-D**). None of the small substituents improved solubility however, this was not unexpected as a majority of the additions increase lipophilicity and hence, were likely to reduce solubility (Figure 14**A-D**). Of all tested compound, only para-fluoro **16a** and trifluoromethoxy **16b** exhibited similar properties to **C38**, retaining both affinity, metabolic stability in both human and mouse liver microsomes, as well as kinetic solubility.

Molecular Modelling

The advances in GPCR crystallization techniques has enabled the AT_2R to be crystalized.[133–135] Using these structures, it is possible to explore the binding cavity of AT_2R. This can be used to both propose the binding mode of known ligands and assist in the design of new ligands. The structure-activity relationship for ligands **16a-e** and **16i-k** could largely be explained by the binding mode proposed for **C38** using a recently published crystal structure[133] of AT_2R (Figure 15). In 2017, Zhang et al. published the crystal structure of AT_2R binding the selective AT_2R antagonist L-161,638.[133,134,140]

A comprehensive docking exploration using the published crystal structure of AT_2R[133], revealed a common binding pose for the ligands **16a-e** and **16i-k** (Figure 15). Elucidating the binding mode revealed the sulfonyl carbamate is anchored via salt-bridge interactions between the sulfone and arginine $182^{4.64}$ and lysine $215^{5.42}$. The carbamate carbonyl forms a hydrogen bond with threonine $125^{3.33}$. The butyl substituent on the sulfonyl carbamate is located in a cavity between the third and the fifth transmembrane helices. The isobutyl group is placed in a deeper region of the transmembrane cavity, defined by the residues leucine, methionine, tryptophan, and two phenylalanines. The phenyl ring is surrounded by tryptophan $100^{2.60}$ and leucine $124^{3.32}$, allowing the imidazole substituent to be accommodated within a hydrophobic cluster composed of four tyrosines, a proline, and an isoleucine. The location of the

phenyl ring reveals that para-substituents added to the ring (**16a-b**, **16d-e**, **16l**) are likely oriented in a cavity pointing towards the extracellular side (Figure 15**A-B**). The reduced affinity of meta och ortho substituents **16i-k** can be explained by a sub-optimal fit of these ligands in the site between arginine $182^{4.64}$ and tryptophan $100^{2.61}$ (Figure 15**D-F**). The retained affinity for meta-fluoro **16c** is likely due to favorable electrostatic interactions with arginine$182^{4.64}$ that ortho-fluoro **16i** cannot achieve (Figure 15**C**).

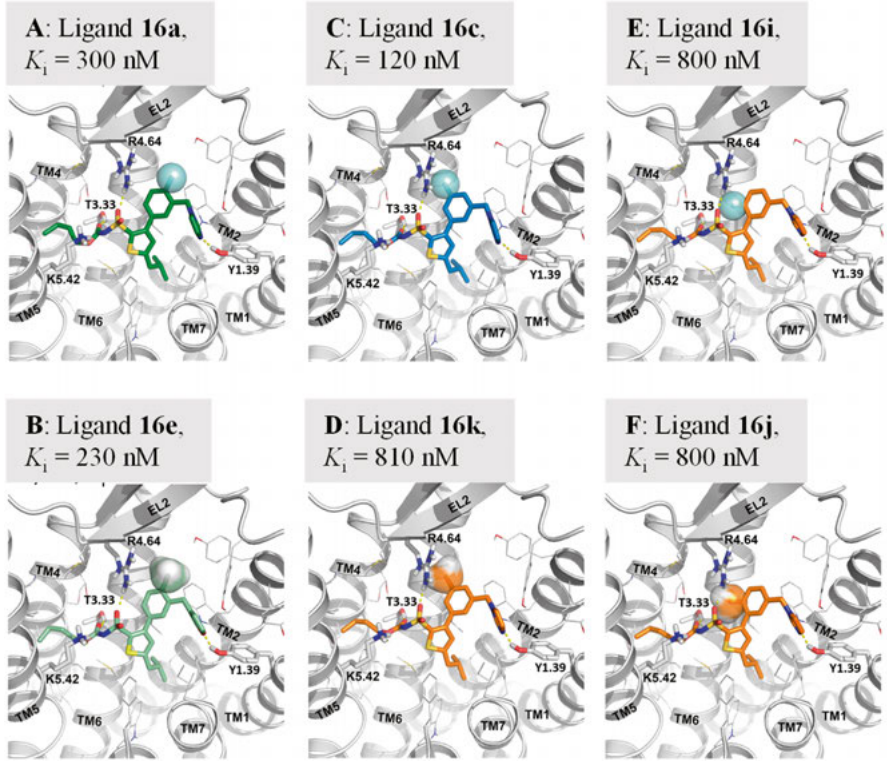

Figure 15. Docked ligands **16a**, **16c**, **16e**, **16i-k** in the most common binding pose in the modeled conformation of human AT_2R.

Synthesis and Evaluation of Bicyclic Analogues (Paper IV)

Strategy

In the final series synthesized to explore the structure-activity relationship of **C38**, the CYP-sensitive imidazole was replaced by bicyclic amides. Previous research by Wan et al. showed that the imidazole ring was important in achieving selectivity for pig AT_2R over rat AT_1R.[63] However, the imidazole ring is a well-established inhibitor of CYP450 enzymes, which are important for drug metabolism.[141] Inhibiting CYP450 enzymes can be very harmful as other drugs taken simultaneously might not be properly metabolized, resulting in unwanted side effects and/or increased risk of toxicity.[142] When **C21** was tested by Mahlingam et al. in 2010 the agonist exhibited high inhibition of CYP450 enzymes 2C9 and 3A4.[143]

Murugaiah et al. replaced the CYP-liable imidazole with amides in their 2012 exploration of the **C38** scaffold.[69] The resulting compounds retained affinity for AT_2R and maintained selectivity over AT_1R. Unfortunately, the inherent metabolic instability of amides make them unfavorable for further development. Evaluating amide **C93** confirmed the metabolic stability in both human and mouse liver microsomes was poor (Figure 7, p.32). Introducing the bicyclic amide allowed the binding orientation of the amide to be ascertained. In addition, cyclization can mitigate phase I metabolism. Attempting to improve the metabolic stability further, the sulfonyl carbamate chain was shortened for a majority of the compounds in the third series, as this had proven favorable in the first series.

Synthetic Work

The general reaction pathway discussed previously (Figure 8-10) was slightly modified to synthesize the bicyclic compounds (Figure 16). For a majority of the ligands in the third series, the amide carbonyl was not included in the bicycle. Acylation and mesylation yielded the isoindolines and isoquinolines **22a-j**. These were subsequently coupled with MIDA boronate **8** using Suzuki conditions. Deprotecting the *tert*-butyl sulfonamide and reacting the primary sulfonamide with either butyl chloroformate or ethyl chloroformate generated the new ligands **23a-k** in moderate to good overall yield.

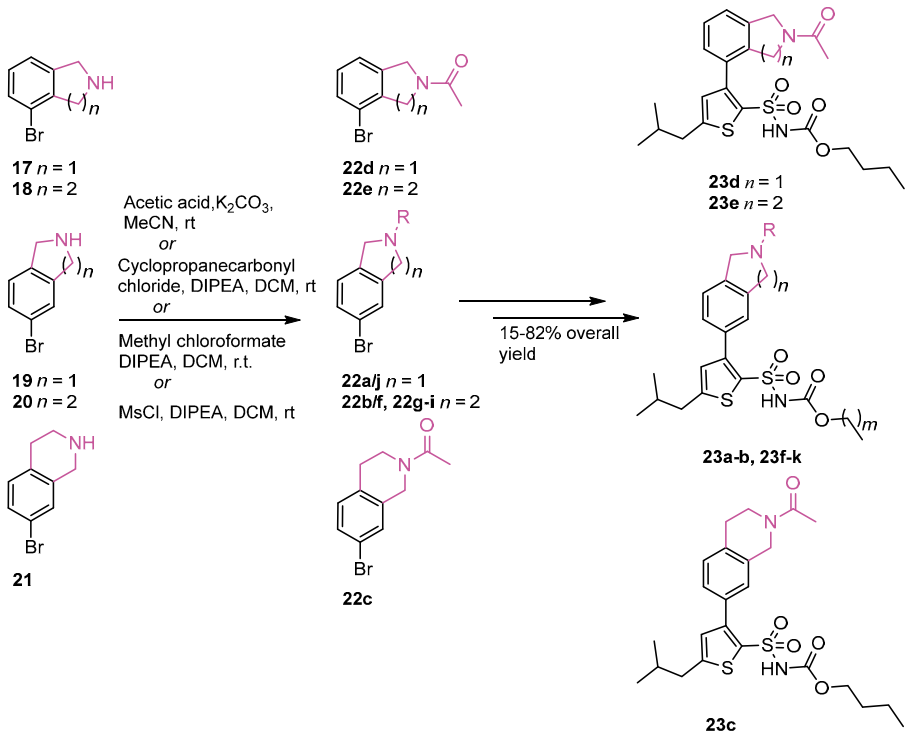

Figure 16. Synthesis of bicyclic analogues. Acylation or mesylation of isoindoline of isoquinolines yielded the intermediated **22a-j**. Following the established synthetic pathway produced 11 new AT_2R ligands (**23a-k**).

Three ligands incorporating the amide carbonyl in the bicycle were synthesized (Figure 17). Reacting bromophenylacetic acid **24** with thionyl chloride and methylamine or ethylamine generated the secondary amides **25a-b**. The Pictet-Spengler condensation/cyclization using paraformaldehyde was employed to cyclize the intermediates to form **26a-b**. The reaction is traditionally performed using polyphosphoric acid, but this was replaced with Eaton's reagent (7.7 wt-% P_2O_5 in $MeSO_3H$).[144,145] Eaton's reagent will activate the carbonyl carbon of the aldehyde, after which the *N*-alkylated amide can attack. Alkylideneacetamide forms after dehydration, and subsequent intramolecular electrophilic aromatic substitution generates the lactams **26a-b**. Lactam **26c** was obtained after dimethylating **26b**. Suzuki coupling with MIDA boronate **8**, deprotecting the sulfonamide, and reacting the primary sulfonamide with ethyl chloroformate produced the new lactam ligands **27a-c** in low to fair overall yields.

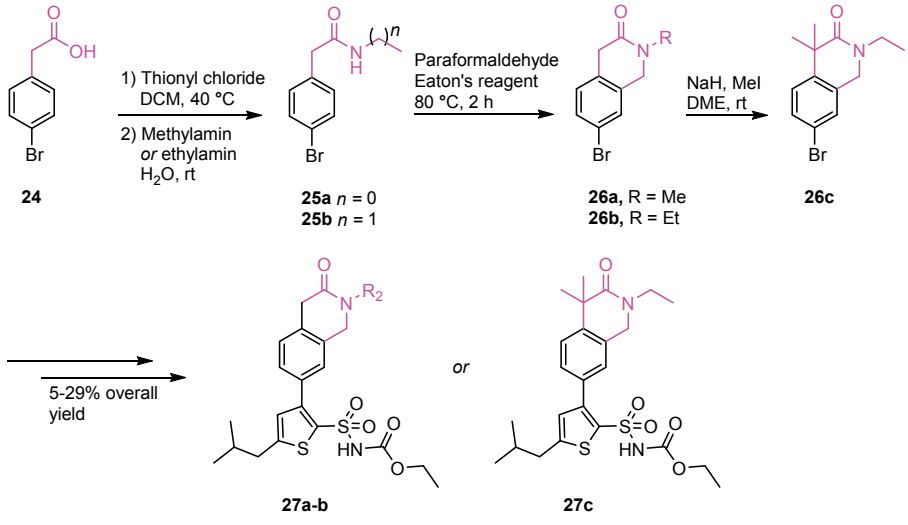

Figure 17. Synthesis of lactam analogues. After generating the secondary amides **25a-b**, a Pictet-Spengler type condensation/cyclization gave the lactam intermediates **26a-b**. Dimethylation of **26b** gave **26c**. Reacting these intermediates according to the established synthetic pathway produced three new AT_2R ligands (**27a-c**).

Results and Discussion

Using the bicyclic amides, the optimal amide orientation could be ascertained and ligands with similar affinity for human AT_2R as **C93** were identified (Figure 18). The bicyclic ligands in the third series retained selectivity for human AT_2R over human AT_1R (data not shown), similar to the first and second series presented in this thesis. As outlined in Figure 18**A**, isoindoline **23a**, and isoquinolines **23b** and **23c** all present with similar affinity to human AT_2R as **C93**. This indicates a favorable amide orientation. Isoindoline **23d** and isoquinoline **23e** confirm the favorable orientation as both exhibit significantly reduced affinity (Figure 18**B**). Kinetic solubility was low for the first five bicyclic ligands investigated. The metabolic stability of these bicyclic amides (**23a-23e**) was low in both human and mouse liver microsomes and unfortunately did not exhibit any improvement compared to the amides **C93**.

Having identified the optimal orientation, additional ligands were synthesized to investigate if the amide could be extended. As the results from the first series presented in this thesis indicate, reducing lipophilicity of the sulfonyl carbamate chain can reduce metabolism. Hence, the butyl carbamate chain was replaced with ethyl carbamate (Figure 18**C-D**). The previously noted tolerability to changes in the sulfonyl carbamate chain did not fully translate to the bicyclic compounds, as shortening the carbamate chain slightly decreased the affinity for human AT_2R (2-fold): **23f** cf. **23b**, and **23j** cf. **23a**.

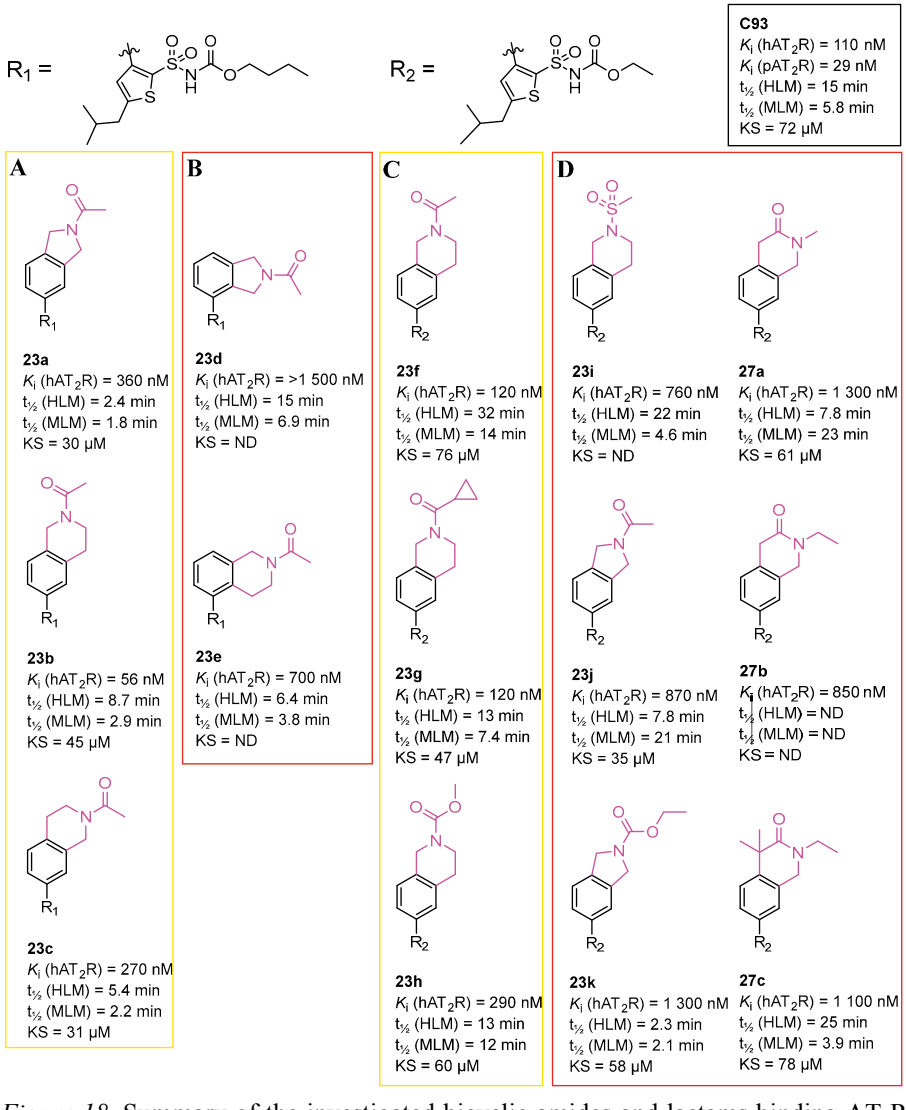

Figure 18. Summary of the investigated bicyclic amides and lactams binding AT_2R selectively. The affinity for human AT_2R (K_i), the metabolic stability in human liver microsomes (HLM) and mouse liver microsomes (MLM), and the kinetic solubility (KS) was determined. **A**) Three compounds with a butyl carbamate chain exhibited similar affinity as **C93**. The kinetic solubility and metabolic stability in both mouse and human microsomes was reduced. **B**) Two ligands exhibited both reduced affinity and metabolic stability. **C**) Three compounds with an ethyl carbamate chain displayed similar affinity as **C93**, with slightly improved metabolic stability. **D**) Six ligands were inferior to **C93** in regards to affinity, metabolic stability, and kinetic solubility.

Introducing a cyclopropyl function or an ester (**23g**, **23h**) produced affinities comparable to **C93** (Figure 18**C**). The mesyl amide **23i** and ethyl carbamate **23k** both exhibited slightly reduced affinity (Figure 18**D**). This indicates the

bicycles could be aligning into a part of the binding cavity that does not allow increasing bulk of the moiety or possibly that the ring size reduction in **23k** produces an unfavorable orientation. Introducing the ethyl carbamate only slightly improved the metabolic stability in human microsomes (**23f-i**), and none of the ligands showed the same properties as **C38** or **13a**/**13b**. As opposed to previous results, the metabolic stability was higher in human than in mouse liver microsomes for a majority of the ligands in the third series. The kinetic solubility remained moderate for all compounds in the third series.

Incorporating the carbonyl amide in the bicycle yielded lactams **27a-c**, which all exhibited low affinity compared to **C93** (Figure 18**D**). Disregarding the low affinity, the metabolic stability profiles of lactam **27a** and **27c** are notable as the former is more stable in mouse microsomes while the latter with higher lipophilicity is more stable in human microsomes. The kinetic solubility was moderate to acceptable for the lactams.

Molecular Modelling

The binding mode of the compounds in the final series was not assessed in the model used to investigate the second series, the substituted phenyl rings. When the amides **C93**, **C97**, and **C102** were first reported in 2012, a selection of the amides presented in the publication were evaluated for functional activity revealing both agonists and antagonists.[69] This indicates a complex pharmacological relationship for ligands deviating from the imidazole head group. Combined with the available crystal structures binding antagonists make molecular modeling precarious. Hence, docking studies of the bicyclic amides were suspended until their functional activity can be evaluated.

Supplementary In Vitro Pharmacology

The IC_{50} values of two of the compounds synthesized, **16a** and **23b** were assessed in an orthogonal second assay using whole cells, performed in a different laboratory (Figure 19). The antagonist **C38** and the agonist **C21** were used as reference. The AT_2R agonist **C21** exhibited an IC_{50} of 1.47 nM for human AT_2R in the orthogonal assay, correlating well with data obtained from the standard assay (K_i = 1.10 nM, membrane preparations). The IC_{50} of **C38** was significantly higher in this orthogonal assay compared to the pig AT_2R assay as well (IC_{50}= 694 nM) but was comparable with the results in the standard assay. A 3-fold improved affinity was noted for para-fluoro **16a** compared to **C38** in this orthogonal assay, which was not observed in the standard assay (**C38**; K_i = 270 nM and **16a**; K_i = 300 nM, respectively). Thus, in the orthogonal assay the selectivity was an estimated 46-fold selectivity for human AT_2R over human AT_1R (cf. 14-fold hAT_1R/hAT_2R selectivity for **C38**). Bicycle **23b** and **C38** exhibit similar IC_{50} values in this orthogonal assay (**C38**; IC_{50}= 694 nM and **23b**; IC_{50} = 818 nM, respectively), although a larger

affinity difference was noted in the standard assay (**C38**; K_i = 270 nM and **23b**; K_i = 56 nM, respectively).

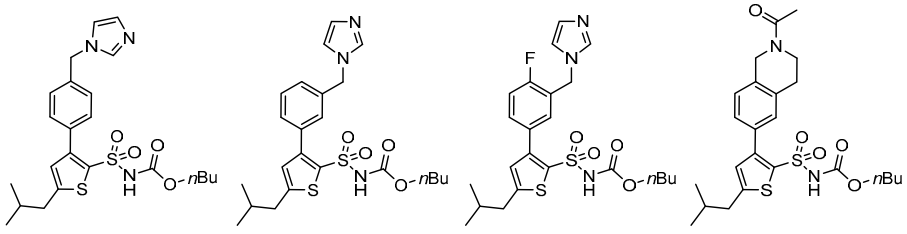

Figure 19. Affinity towards human AT_2R for selected ligands in the orthogonal assay.

Summary of the Structure-Activity Studies of **C38** and Future Outlook

The first series identified the sulfonyl carbamate as a site allowing large variability, and also proved important for phase I metabolism. The sulfonyl carbamate moiety was explored using the quick, simple, and safe transesterification of sulfonyl carbamates presented previously in this thesis. Additional sulfonylureas and acyl sulfonamides were evaluated as possible replacement of the sulfonyl carbamate moiety, but neither presented with improved properties compared to **C38**. In contrast to previous knowledge, a flat structure-activity relationship was observed with a notable broad tolerability to changes. The key finding was the significantly improved in vitro metabolic stability when shortening the carbamate alkyl chain. Compounds **13a** and **13b** exhibited similar affinity as **C38** and improved stability in mouse microsomes, making them suitable research tools for mouse models of neuropathic pain.

The second series revealed that the phenyl ring is likely not the main site for phase I oxidation, and with the compounds generated a proposed binding mode of **C38** was ascertained. Introducing small substituents was fairly well tolerated, rendering seven compounds with maintained human AT_2R affinity. Adding fluoro substituents to the phenyl ring did not improve metabolic stability, and exchanging the phenyl ring for a pyridine did not improve solubility. The common binding pose of the ligands in the AT_2R crystal structure could explain the experimental affinities: adding substituents in the ortho or meta position relative to the thiophene will result in sub-optimal fitting between arginine 182 on the forth transmembrane helix and tryptophan 100 on the second transmembrane helix.

In the final series, the imidazole of **C38** was replaced with bicyclic amides and lactams, adding insight into the structure-activity relationship of the amide moiety. The optimal amide orientation was identified, generating the most potent of all ligands presented in this thesis, isoquinoline **23b**. Rapid decomposition was noted which is unfortunate as both the amides and the bicyclic amides could have mitigated the risk of CYP450 enzyme inhibition posed by the imidazole containing ligands.

In summary, the three series of selective human AT_2R ligands synthesized and evaluated have broadened the structure-activity knowledge of the **C38** scaffold, Figure 20. The transesterification proved a useful reaction to generate biologically active compounds, for which the metabolic stability was improved. This knowledge might be useful to improve stability of other AT_2R ligands. The effect was not translatable to the bicyclic amides, which are likely more metabolically labile due to the bicyclic amide moiety itself. In future projects the bicyclic ligands might help to further elucidate the pharmacological profile of AT_2R ligands and could improve our understanding of the structure-functional relationship.

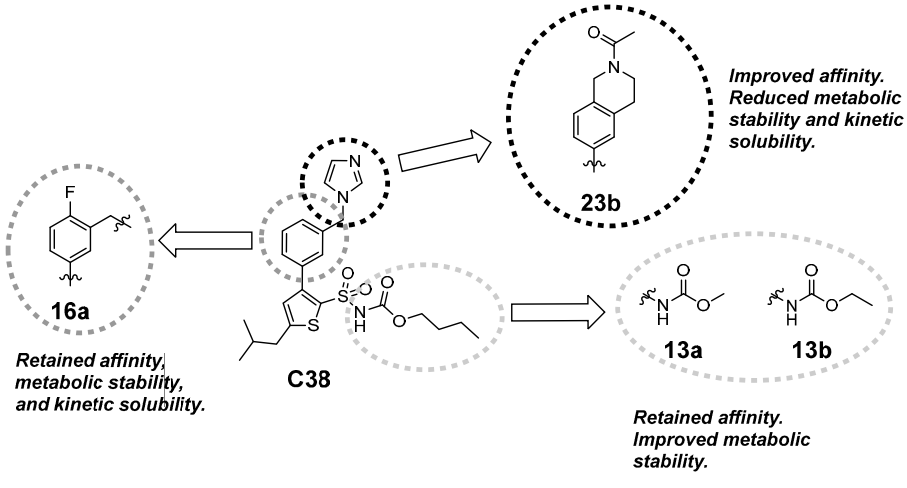

Figure 20. Summary of the most favorable improvements to the **C38** scaffold.

Investigation of NO release in Macrophages as a Functional Activity Indicator for AT_2R Ligands (Paper V)

Background and Strategy

The biological response and potential use of AT_2R ligands is greatly dependent on the ligand's functional activity. The low basal expression of AT_2R in combination with poorly understood signaling pathways, make determining an AT_2R ligand's functional activity a formidable challenge. When the first reported selective non-peptide AT_2R agonist **C21** was presented in 2004, its agonist activity was determined using two assays.[63] In an in vivo bicarbonate secretion assay, the alkaline secretion in rat duodenum was determined using continuous titration with diluted hydrochloric acid.[63,146] Testing **C21** in a neurite outgrowth assay confirmed the agonist activity exhibited by the ligand. Undifferentiated cells of the hybrid cell line NG108-15 (mouse neuroblastoma × rat glioma) were subjected to a 3-day treatment with AT_2R ligands to induce neurite outgrowth. Using contrast microscopy the percent of cells with neurites longer than a cell body, out of the total amount of cells in the picture, was determined.[147–149] Although a large number of AT_2R ligands have been disclosed over the past two decades[95–98,150], functional activity has only been determined for a selected few. The most notable being **C38**, displaying antagonistic properties in the neurite outgrowth assay.[99] Both presented assays do not allow a large throughput of ligands due to high cost and time requirements. Attempts to restart the neurite outgrowth assay were unsuccessful and thus, identifying a new assay was a high priority. Together with the Fändriks group at Sahlgrenska Akademin, I set out to identify a suitable assay that would allow a higher throughput, and to evaluate the assay with known AT_2R ligands.

Macrophages and AT_2R

Several research groups have investigated the anti-inflammatory function exerted by AT_2R in macrophages. Macrophages are highly plastic cells vital to an organism's development, tissue remodeling and repair, and immune response. Resident macrophages are present in all tissues where they partake in tissue homeostasis. Circulating monocytes will be recruited into tissue in

response to metabolic, inflammatory, or immune stimuli. The micro-environment in the tissue determines the differentiation of the diffusing monocytes to macrophages. There are several classification systems based on function used to describe macrophages, encompassing both reversible differentiation and several proposed sub-categories. In the classical definition, the activated macrophages (CAMs, or M1) are pro-inflammatory, while the alternatively activated macrophages (AAMs, or M2) are anti-inflammatory.

Stimuli with interferon-gamma (INF-γ) or activation of a toll-like receptor (TRL) will result in M1 phenotypic differentiation of macrophages.[151–153] Lipopolysaccharide (LPS) will stimulate an acute inflammatory response in macrophages, causing M1 phenotypic differentiation and resulting in nitric oxide (NO) production (Figure 21). LPS binds to the TLR4 resulting in downstream upregulation of nuclear factor κβ (NF-κβ), in turn regulating the expression of inflammatory cytokines, tumor necrosis factor-α (TNF-α), and inducible NO synthase (iNOS). The NO production derives from L-arginine (L-Arg) as iNOS converts it to L-citrulline. Direct stimulation of AT_2R in LPS-triggered macrophages has been shown to inhibit NF-κβ and attenuate cytokines interleukin (IL) 6 and IL-10 as well as TNF-α. Stimulation of AT_1R has been shown to exhibit the opposite effect.[154–157] Hence, a negative modulation of NO in LPS activated M1 phenotypic macrophages could be an indication of an agonistic character of a selective AT_2R ligand.

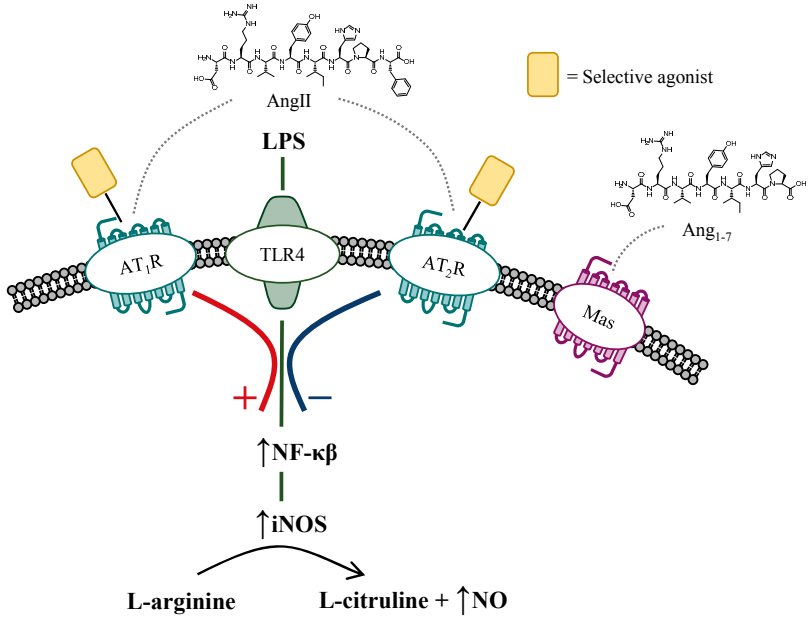

Figure 21. Proposed effect of AT_2R and AT_1R activation on NO production in LPS-triggered macrophages.

Cell Validation and Basal Protein Expression

In the first experiments, the objective was to confirm the basal expression of important proteins in the M1 phenotypic RAW264.7 mouse macrophages (Figure 22**A**). Treating the cells with or without LPS for 16 h and analyzing the protein presence according to standard Western blot protocols, confirmed that the cells expressed all the desired proteins (AT_1R, AT_2R, iNOS, and NF-κβ). Next, the macrophages were validated with varying LPS stimuli for 16 h, to confirm a dose-dependent response of NO. The nitrite (NO_2^-) concentration in the supernatant was determined using Griess reagent as an indicator of NO production, and a dose-dependent response was observed (Figure 22**B**). The LPS-triggered macrophages (16 h stimuli) were washed and treated with LPS-free medium for 2, 4, and 6 h. The nitrite levels were determined at each time point (Figure 22**C**). At the lower doses of LPS (1 and 10 ng/mL), the NO production was low and unstable, while the higher doses (50 and 100 ng/mL) gave apparent dose-dependent responses. This indicates that for the higher LPS doses the macrophages retain their phenotypic differentiation for up to 6 h after discontinuing TLR4 stimulation. Cells in passage 5-23 were identified as phenotypically stable, a trend supported by data presented by Taciak et al. in 2018.[158]

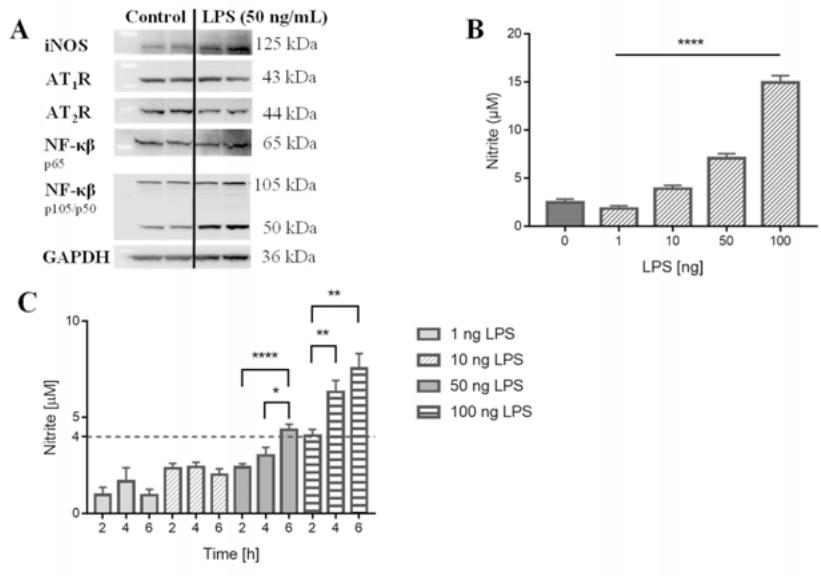

Figure 22. The RAW264.7 macrophages were validation to confirm M1 phenotypic expression. **A**) Immuno-blot analysis of basal expression of iNOS, AT_1R, AT_2R, and NF-κβ; GAPDH served as a loading control **B**) Dose-dependent effect of LPS on nitrite levels (indirect measure of NO release) in macrophages stimulated for 16 h. **C**) Time-dependent effect on nitrite levels in macrophages after removal of LPS. ****p<0.0001; **p<0.01; *p<0.05; data is presented as mean±SEM, one-way ANOVA followed by two-tailed Student's t-test (B: n=9-15; C: n=6-7).

Evaluating the Assay with AT_2R Ligands **C21** and **C38**

Effect of AT_2R Ligands **C21** and **C38** in LPS-Differentiated Macrophages

Treating LPS-triggered RAW264.7 macrophages with the selective AT_2R agonist **C21** reduced the nitrite levels as hypothesized. The RAW264.7 macrophages were stimulated with LPS for 16 h to trigger M1 phenotypic differentiation. Subsequent treatment with AT_2R agonist **C21** for 6 h in LPS-free medium resulted in attenuation of NO production (Figure 23**A**). However, the agonist did not display a linear dose-response relationship in this set-up, and plateaued at 60-70 μM nitrite for 10, 50, and 100 μM of **C21**. Although it is possible that the higher doses of **C21** cause internalization of the protein, terminating the LPS stimulation of TRL4 would likely result in down-regulation of NF-κβ. In turn, this could initiate a negative feedback-regulation decreasing the expression of AT_1R and AT_2R at (or near) the cell surface.

Please note that the selective AT_2R agonist **C21** has opposing effects on NO production depending on the tissue. In 2018, Peluso et al. reported that stimulating human aortic endothelial cells (HAEC) with **C21** caused increasing NO levels via endothelial NO synthase (eNOS). The vasodilating effect exhibited by AT_2R results from NO release in endothelial cells.[159] Although the eNOS and iNOS signaling pathways are different, it is interesting to note the vastly different effect AT_2R agonist **C21** exhibits on NO production in endothelial cells and macrophages.

The agonistic effect of **C21** could be almost completely blocked by pretreating the LPS-triggered macrophages for 1 h with the established prototype antagonist **PD123,319** (Figure 23**B**, structure Figure 4, p.16). A 20% recovery in NO production was observed for the lowest dose of **C21** when pretreating with **PD123,319**. This recovery was not observed when increasing the dose of **C21** while keeping the **PD123,319** concentration constant. It is possible that the slight difference in affinity between the two ligands (IC_{50} **C21** = 2.3 nM cf. IC_{50} **PD123,319** = 5.6 nM)[160], in combination with reduced AT_2R expression, results in only a 10-fold excess of **PD123,319** successfully reducing the **C21** effect.

Treating the M1 phenotypic macrophages with the AT_1R selective antagonist Losartan or the Mas receptor antagonist A779 showed no statistically significant effect on the NO reduction (Figure 23**C**) indicating the observed effect of **C21** is mediated via AT_2R. The Mas receptor agonist AVE0991 and AT_2R agonist **C21** are structurally similar, differing mainly in the imidazole head group (structure not shown).[161] There is also evidence for heterodimerization between AT_2R, and AT_1R or the Ang_{1-7}-sensitive Mas receptor. The functional effect of this complex heterodimerization, and/or the occurrence of it, seem dependent on both tissue and cell type.[161–164] In 2017, Leonhardt et al. observed cross-inhibition of AT_2R with a Mas receptor

antagonist, similar to the cross-inhibiting effect upon AT_1R/AT_2R dimerization observed by AbdAalla et al. in 2001.[162,164] To confirm the effect of **C21** on macrophages was mediated via AT_2R, and to investigate if there was any cross-inhibition in the system, the LPS-triggered macrophages were pretreated with Losartan or A779 for 1 h, after which **C21** was added to the cells. Neither experiment showed any significant preventive effect on the **C21**-derived NO attenuation, indicating the reducing effect of **C21** is mediated via AT_2R and is not affected by cross-inhibition in this system.

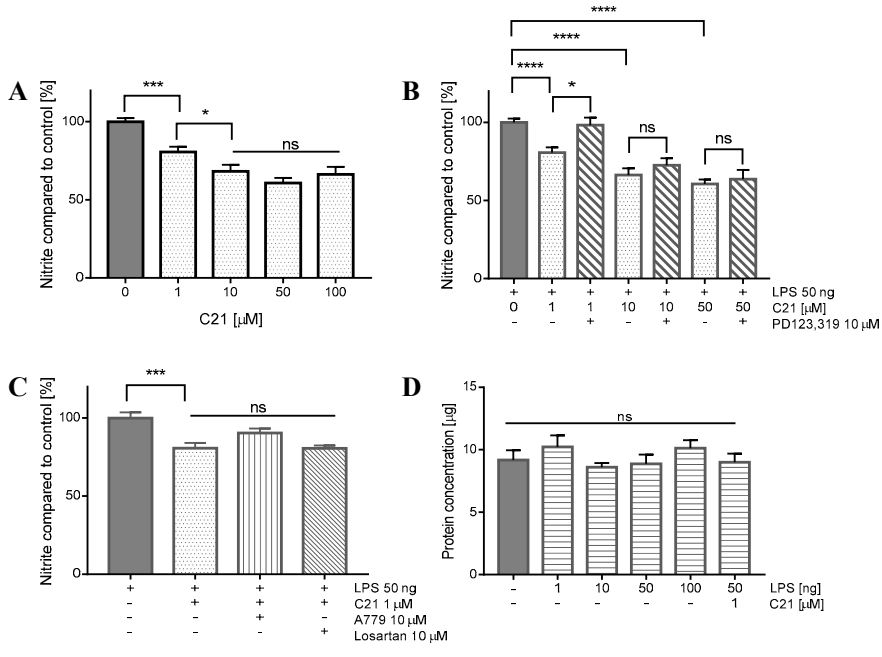

Figure 23. The effect of the AT_2R agonist **C21** on NO production in M1 phenotypic macrophages. **A**) NO production in macrophages incubated with 50 ng/mL LPS for 16 h, and subsequently incubated with **C21** (1-100 µM) in LPS-free medium for 6 h. **B**) The effect of **C21** 1 µM could be blocked by pretreatment with **PD123,319** for 1 h, while the effect of **C21** 10 and 50 µM could not. **C**) The effect of **C21** 1 µM could not be blocked by pretreatment for 1 h with neither receptor Mas antagonist A779 nor AT_1R antagonist Losartan. **D**) The protein concentration measured with the Bradford method. ****p<0.0001; ***p<0.001; *p<0.05; ns = no significance (p>0.05); data is presented as mean±SEM, one-way ANOVA followed by two-tailed Student's t-test (A: n=8-47; B: n=12-28; C: n=3-28; D: n=2-5).

The cells remained viable throughout the experiments. Ocular inspection showed the cells grew and remained semi-adherent. The protein concentration was determined using the Bradford method. The tested macrophages all exhibited stable protein levels through a variety of experiments, confirming cells remained viable even after LPS and **C21** treatment (Figure 23**D**).

The AT_2R prototype antagonist **C38** shows agonistic properties in M1 phenotypic RAW264.7 macrophages. When treating the M1 phenotypic macrophages with the reported antagonist **C38** for 6 h, an *agonist* typical attenuation of NO production was observed (Figure 24**A**). Pretreating the cells for 1 h with **PD123,319** resulted in complete recovery of nitrite levels, confirming the surprising agonistic character of **C38** (Figure 24**B**). When first reported[69], **C38** was tested in the neurite outgrowth assay and displayed antagonist behavior. While it cannot be excluded that different signal pathways in NG108-15 cells and M1 macrophages result in varied functional activity, it is plausible that limitations in the neurite outgrowth assay did not allow partial agonistic properties to be discerned. Using partial agonists rather than antagonists can be very useful to reduce the effect of a full agonist, as mentioned in the *Introduction* (p. 12). Hence, **C38** and its analogues may lead to useful applications in future drug discovery programs.

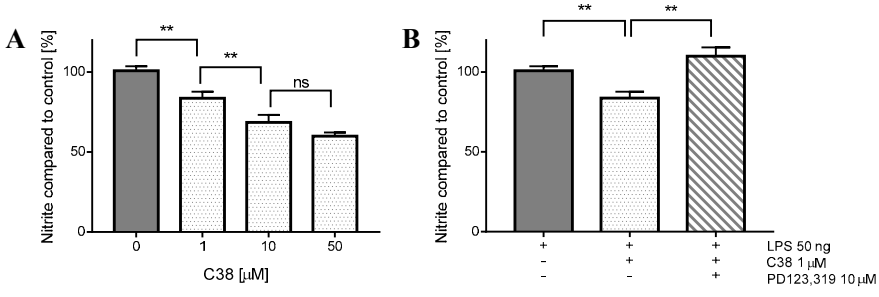

Figure 24. The effect of the AT_2R agonist **C38** on NO production in M1 phenotypic macrophages. **A**) NO production in macrophages incubated with 50 ng/mL LPS for 16 h, and subsequently incubated with **C38** (1-50 μM) in LPS-free medium for 6 h. **B**) Pretreatment with **PD123,319** for 1 h could block the effect of **C38**. $**p<0.01$; ns = no significance ($p>0.05$); data is presented as mean±SEM, one-way ANOVA followed by two-tailed Student's *t*-test (n=6-9).

Effect of **C21** on Macrophages During Simultaneous Macrophage Differentiation

In the second protocol evaluated, the agonist **C21** exhibited a linear dose-dependent attenuation of NO production. Undifferentiated macrophages were treated for 16 h with **C21** and simultaneously activated using a low dose of LPS to initiate phenotypic differentiation. The inhibitory effect at the lowest dose **C21** remained the same as in the first protocol. The inhibitory effect became more pronounced for the higher doses of **C21**, resulting in a linear dose-response relationship (Figure 25**A**). Although, loss of viability could explain this effect, the cells remained semi-adherent for all tested doses and the protein levels were unchanged (Figure 25**B**). The results support the previously presented hypothesis, that continued LPS activation of TLR4 likely

result in AT_2R remaining expressed at (or near) the cell surface. Pretreating the cells for 1 h with **PD123,319** was again only successful in inhibiting the lowest dose of **C21**, possibly caused by the difference in affinity between **C21** and **PD123,319** (Figure 25**C**).

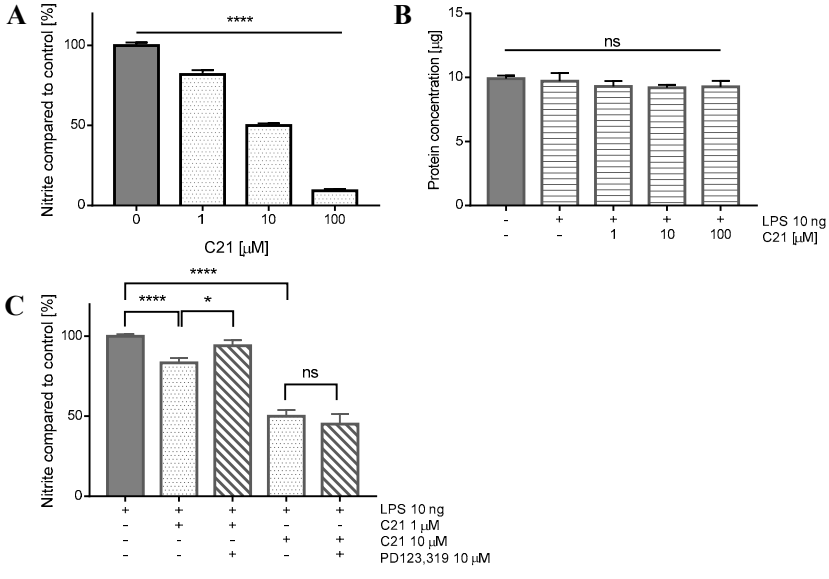

Figure 25. The effect of the AT_2R agonist **C21** on NO production in M1 phenotypic macrophages, after simultaneous stimulation with a low dose of LPS. **A**) NO production in macrophages incubated with 10 ng/mL LPS and **C21** at varying doses (1-100 μM) for 16 h. **B**) The protein concentration measured with the Bradford method. **C**) The effect of **C21** 1 μM could be blocked by pretreatment with **PD123,319** for 1 h, while the effect of **C21** 10 μM could not be blocked. ****p<0.0001; *p<0.05; ns = no significance (p>0.05); data is presented as mean±SEM, one-way ANOVA followed by two-tailed Student's t-test (A: n=6-15; B: n=9-24; C: n=4-9).

Effect of AT_2R Ligands **C21** and **C38** in Highly Stimulated Macrophages

Treating highly stimulated macrophages with AT_2R ligands **C21** and **C38** attenuate NO production, confirming the agonistic character of both these ligands. In the third protocol, the macrophages were pretreated with AngII for 1 h before stimulating the cells for 16 h with AngII, a high dose LPS, and **C21** or **C38**. Both ligands decreased nitrite levels in a sigmoidal dose-dependent response, confirming the agonistic function of ligands **C21** and **C38** in RAW264.7 macrophages (Figure 26**A**). The higher doses (50 and 100 μM) resulted in almost complete attenuation of NO production. This is probably related AT_2R surface expression resulting from LPS triggering TRL4. The

addition of AngII may also result in increased recruitment of AT_2R to (or near) the cell surface, increasing the response of **C21** and **C38**.

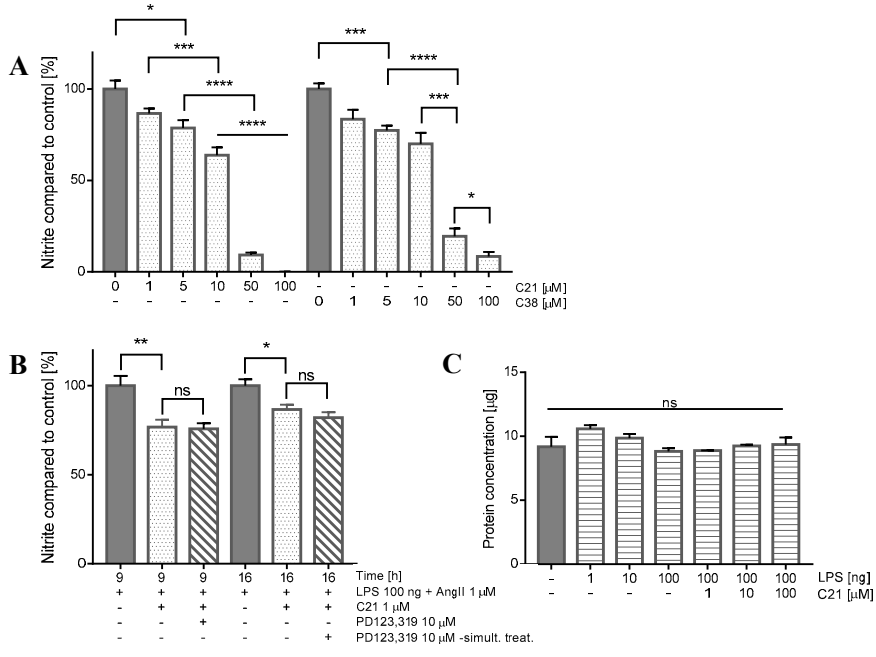

Figure 26. The effect of AT_2R agonist **C21** on NO production in M1 phenotypic macrophages, after simultaneous stimulation with AngII and a high dose of LPS. **A**) NO production in AngII-pretreated macrophages incubated with 100 ng/mL LPS and **C21** or **C38** at varying doses (1-100 μM). **B**) The effect of **C21** 1 μM was unaffected by co-treatment with 10 μM **PD123,319**. **C**) The protein concentration measured with the Bradford method. ****p<0.0001; ***p<0.001; *p<0.05; ns = no significance (p>0.05); data is presented as mean±SEM, one-way ANOVA followed by two-tailed Student's t-test (A: n=3-12: B: n=7-18; C: n=2-9).

Co-treating the cells with the established AT_2R antagonist **PD123,319** and **C21** showed no inhibitory effect on the NO production in the highly stimulated macrophages (Figure 26**B**). While the simultaneous addition of the drugs may explain this trend, additional experiments with pretreatment of **PD123,319** exhibited the same trend (cells treated for 9 h). The presence of endogenous AngII could explain this effect since its affinity is higher than that of **C21**, and both **C21** and AngII will compete with **PD123,319**.[160] Although AngII is present in low levels in all our experiments in the cell culture medium, the combination of **C21** and increased levels of AngII could outcompete **PD123,319** in the highly stimulated macrophages. AngII also activates both AT_1R and AT_2R, and could be degraded into peptides with down-stream activity in RAAS (e.g. Ang_{1-7} binding the Mas receptor). However, treating the macrophages with the AT_1R selective antagonist Losartan or the Mas

receptor antagonist A779 according to the first protocol revealed no effects on the NO production, indicating there is likely no other activity in RAAS.

Despite the major changes observed in NO production, the protein concentrations remained unchanged and comparable to the levels detected in the previous protocols (Figure 26**C**).

Summary and Future Outlook

Studying the effect of AT_2R ligands on the NO release in LPS-treated RAW264.7 macrophages appears to be a feasible biological assay to determine an AT_2R ligand's functional activity. The established AT_2R agonist **C21** and antagonist **PD123,319** confirm that selectively activating AT_2R will attenuate NO production, while the antagonist will inhibit this attenuating effect. Although all three protocols tested would allow higher throughput of ligands than the previously used assay, the linear dose-response to drugs in macrophages simultaneously treated with a low dose of LPS make this protocol the most appropriate for future ligand testing. The first protocol, in which the macrophages were pretreated with LPS, a linear dose-response was lacking probably due to a reduced AT_2R expression. In the third, highly stimulated, protocol the inability to block the agonistic effect of **C21** with **PD123,319** is problematic and may result in both false positives and false negatives.

The reported antagonist **C38** exhibits agonist effects in RAW264.7 macrophages. When first reported, ligand **C38** had been tested in a neurite outgrowth assay indicating the ligand acted as an antagonist. In the LPS-triggered macrophages, the ligand instead presents with agonist properties. While the ligand may exhibit different functional activity in different cell types and pathways, it is more probable that limitations in the neurite outgrowth assay could not discern a partial agonist activity of **C38**. As mentioned in the *Introduction* of this thesis (p. 12), partial agonist can be useful drugs. With the assay presented in this thesis, more ligands can be evaluated for functional activity, which will help further elucidate the relationship between function and structure for AT_2R ligands.

Several studies conclude that AT_2R activation results in an anti-inflammatory response, in correlation with our finding.[154–156,165] However, in 2018, Shepard et al. presented data in contrast to this previous research, concluding that AT_2R *activation* in macrophages triggers production of reactive oxygen/nitrogen species (ROS/RNS, i.e. nitric oxide). The authors investigated the effect of the clinical candidate AT_2R antagonist **EMA401** (structure Figure 7, p. 16) and found its effect to be mediated via macrophages infiltrating the injured nerves. Previous research has proposed the effect of **EMA401** to be a direct interaction with AT_2R in the damaged nerves.[166,167] Shepard et al. found that the nerves do not express AT_2R, as opposed to

previous suggestions presented in the literature and briefly mentioned in the *Introduction* of this thesis (p. 17). Further, the authors discovered that increased levels of ROS/RNS cause cysteine modification of the transient receptor potential ankyrin 1 (TRPA1) channel in DRG sensory neurons, resulting in increased hypersensitivity. Blocking AT_2R activation reduced ROS/RNS and in turn reduced hypersensitivity. This contrasts with the findings that AT_2R activation in RAW264.7 macrophages decreases the levels of NO. While the generalizability of in vitro and in vivo data is highly limited, these opposing results highlight the complex biological function of AT_2R. Work is ongoing with the RAW264.7 macrophage assay to evaluate the clinical candidate **EMA401** and discern its effect in the system.

Concluding Remarks

This thesis outlines the design and synthesis of ligands relating to the **C38** scaffold with the purpose of evaluating the structure-activity relationships and identifying motifs important to improving the drug-like properties of the reported antagonist. Presented below are the main conclusions.

- A new reaction to transform a sulfonyl carbamate, a transesterification of sulfonyl carbamates, was identified and successfully explored in both microwave batch and in a microwave heated continuous-flow system.
- Shifting from a displacement assay using pig AT_2R to human AT_2R when determining affinity resulted in a significantly reduced affinity for **C38** but not for **C21**.
- The affinity could only be marginally improved for the compounds containing the imidazole head group.
- The metabolic stability could be improved by reducing the lipophilicity of the carbamate alkyl chain, generating compounds **13a** and **13b**. Both these ligands could be useful tools in mouse models of neuropathic pain.

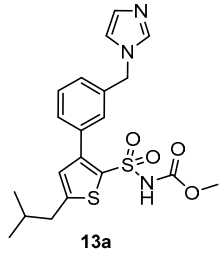

13a
K_i (hAT_2R) = 400 nM
$t_{½}$ (HLM) = 77 min
$t_{½}$ (MLM) = 220 min

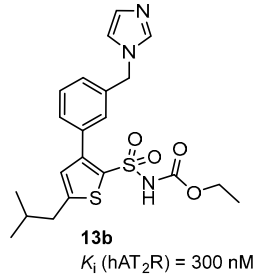

13b
K_i (hAT_2R) = 300 nM
$t_{½}$ (HLM) = 61 min
$t_{½}$ (MLM) = 180 min

- The phenyl ring does not appear to be a main a site for phase I metabolism as adding small substituents onto the ring could not improve the metabolic stability.
- Adding small substituents to the phenyl ring enabled fine-tuning of the binding mode of **C38** in a recently published crystal structure. The para position relative to the thiophene point out toward the extracellular side and additions in this position can be accommodated. For the meta or ortho

positions an addition cannot be accommodated and result in a sub-optimal fit of the ligand.

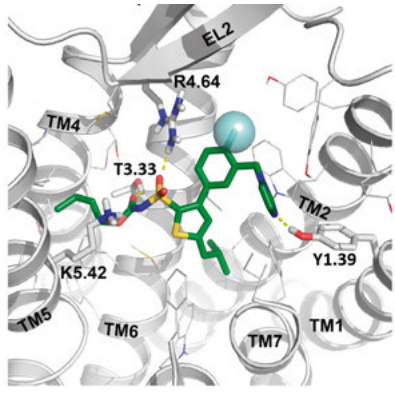

- The amides **C93**, **C97**, and **C102** exhibited similar affinity to human AT_2R in the new assay as **C38**. The metabolic stability was unfortunately poor for these ligands.
- The metabolic stability was only marginally improved by cyclizing the amides, and reducing the lipophilicity of the carbamate chain did not improve the stability to as great extant as seen for the imidazole analogues.
- Exchanging the amides for bicyclic amides allowed the most favorable amide orientation to be elucidated, generating the most potent compound presented in the study, compound **23b**.

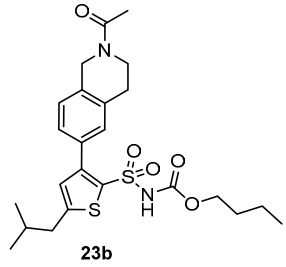

23b
K_i (hAT_2R) = 56 nM
$t_{½}$ (HLM) = 8.7 min
$t_{½}$ (MLM) = 2.9 min
KS = 45 µM

- Investigating the effect of AT_2R ligands on the production of nitric oxide in LPS-triggered RAW264.7 macrophages can be used to evaluate an AT_2R ligand's functional activity.
- Reported antagonist **C38** and confirmed agonist **C21** both reduce the nitric oxide production in RAW264.7 macrophages suggesting **C38** acts as a partial agonist in macrophages.

Populärvetenskaplig Sammanfattning

Inom den moderna medicinen spelar läkemedel en central roll för att behandla eller bota sjukdomar. Forskning kring nya möjliga läkemedel sker främst inom läkemedelsindustrin men till viss del i akademiska projekt. Trots det stora antalet projekt som startas i syfte att identifiera ett läkemedel som skulle kunna behandla eller bota en sjukdom, är det få läkemedelsprojekt som lyckas. Processen är både lång och kostsam, och kombinerat med den höga andelen projekt som misslyckas blir priset på de läkemedel som når marknaden oftast mycket hög.

Läkemedelskemi används för att göra, syntetisera, nya ämnen som är biologiskt aktiva, dvs. som har en effekt på ett biologiskt system och därmed skulle kunna agera som ett läkemedel. Innan kemister kan börja syntetisera biologiskt aktiva ämnen, även kallat substanser eller molekyler, är det viktigt att veta vad substansen kan binda till i ett biologiskt system. De biologiskt intressanta entiteterna som en läkemedelsmolekyl kan binda till är oftast humana proteiner, även om det också finns en del läkemedel som interagerar med t.ex. DNA. Läkemedel kan också interagera med icke-humana proteiner i virus eller bakterier. Det är viktigt att substansen binder så selektivt som möjligt till ett protein som är biologiskt intressant. När ett läkemedelsprojekt starts kan det börja med att flera substanser testas mot biologiskt intressanta proteiner för att identifiera bra startmolekyler, vilken sjukdom som ska behandlas blir då ett sekundärt val. Ett projekt kan även börja med att sjukdomen väljs primärt, och molekyler designas för att binda till ett protein som är vitalt för den sjukdomen.

Högt blodtryck är en mycket vanlig åkomma som biologiskt orsakas av överaktivitet i ett biologiskt system som kallas renin-angiotensin-aldosteron systemet, förkortat RAAS. De första proteinerna i RAAS upptäcktes redan i slutet av 1800-talet, det dröjde dock till mitten på 1970-talet innan den molekyl som utövar den blodtryckshöjande effekten identifierades: en åtta-aminosyror lång peptid kallad angiotensin II (AngII). Det finns idag flera läkemedel som interagerar med proteiner i RAAS som ett sätt att behandla högt blocktryck och minska risken för hjärtkärl-sjukdomar. Under de senaste två decennierna har en skyddande del av RAAS upptäckts. Denna skyddande del innehåller mindre kända protein som utövar bland annat en blodtryckssänkande effekt, men vissa protein har även visat sig kunna vara både nervskyddande och nervregenererande. Ett sådant protein är angiotensin II typ 2 receptorn, ofta förkortad AT_2R.

Proteinet AT_2R är en receptor som sitter bundet i cellmembranet. När receptorn binder AngII på utsidan av cellen kommer proteinet att binda till ett annat protein på insidan, ett G-protein. På så vis förs den extracellulära signalen vidare inuti cellen och leder till att cellen förändrar sitt uttryck av diverse proteiner. Det finns just nu en läkemedelskandidat i kliniska studier, EMA401, som binder till AT_2R och blockerar proteinet från att binda några extracellulära signaler. Det finns studier som indikerat att AT_2R är involverad i neuropatisk smärta och i de kliniska studierna med EMA401 har den upplevda smärtan minskats hos testpersonerna.

Kronisk smärta drabbar en betydande del av befolkningen och är smärta som inte går att bota och vars biologiska orsak oftast är okänd. Kronisk smärta kan uppstå på grund av skador som drabbar nerverna och kallas då neuropatisk smärta. När nerver skadas fysiskt eller på grund av ett annat sjukdomstillstånd (t.ex. diabetes, cancer, virus etc.) kan neuropatisk smärta ibland uppstå. Nerven hamnar då i ett tillstånd av hyperaktivitet, vilket kan leda till att nerven reagerar med smärtsignaler för yttre stimuli som inte är smärtsamt eller att nerven konstant skickar smärtsignaler trots att inget yttre stimuli finns. Idag finns ingen behandling som kan återställa nerverna, utan bygger på dämpning av den upplevda smärtan. Behandlingen är otillräcklig och patienter får inte alltid hjälp av de mediciner de ordineras. Att identifiera substanser som kan hjälpa dessa patienter är av stort intresse.

I vår forskargrupp finns lång erfarenhet av att syntetisera och utveckla substanser som binder till AT_2R. Med det nyvunna intresse som finns för substanser som blockerar AT_2R initierades mitt doktorandprojekt kring substansen **C38**, Figur 27 nedan. För att undersöka vilka delar av en molekyl som är viktiga för dess biologiska effekt undersöks varje del separat. **C38** är en substans som upptäcktes 2012 och bara den övre delen, nedan markerad med en svart ring, har undersökts ytterligare. Den biologiska metod som används för att utvärdera tidigare substanser (baserad på vävnad från gris) var inte längre tillgänglig. Den nya metod vi använde oss av i de arbeten som presenteras i denna avhandling är baserad på vävnad som uttrycker det humana proteinet. Denna metod visade inte samma resultat som den tidigare metoden. Syftet med det arbete som presenteras i denna avhandling blev därför att undersöka tre delar av molekylen **C38** (Figur 27) för att dels försöka identifiera substanser med bättre biologisk aktivitet än **C38**, samt dels att försöka identifiera biologiskt mer stabila substanser. Det arbete som ligger till grunder för de resultat som presenteras i den här avhandlingen är presenterat i fem vetenskapliga arbeten.

Det första och andra arbetet beskriver en viktig del av läkemedelskemi: att utveckla nya kemiska omvandlingar som kan användas för att syntetisera nya molekyler. Den kemiska funktionalitet som återfinns i del I (Figur 27) undersöktes genom att reagera en testsubstans som bär denna funktionalitet, med olika alkoholer vid förhöjd temperatur. Reaktionen fungerade väl för flertalet alkoholer och reaktionen användes i det tredje arbetet för att utforska

del I. Ingen av de 18 nya molekyler som syntetiserades var mer biologiskt aktiv än **C38**, men två substanser med en kortare kedja i denna position visade mycket bättre biologisk stabilitet. I det fjärde arbetet syntetiserades 12 nya substanser för att utforska del II av **C38**. Av de syntetiserade substanserna var det enbart 2 molekyler som var jämförbara med **C38** sett till både biologisk aktivitet och stabilitet. I det fjärde arbetet syntetiserades 14 bicykliska substanser. Efter att ha identifierat den optimala orienteringen av bicykeln erhölls en substans som var mer biologiskt aktiv än **C38**. Dessvärre var dess biologiska stabilitet fortsatt lägre än **C38**, vilket inte förbättrades av en kortare kedja i position I.

Att kunna avgöra om en substans blockerar eller aktiverar AT_2R, dess biologiska funktion, är såklart mycket viktigt för att kunna avgöra dess biologiska användbarhet. Därför startades ett delprojekt med professor Lars Fändriks grupp vid Sahlgrenska akademin i syftet att identifiera en biologisk modell som kunde besvara denna fråga. Genom att använda makrofager, en vital celltyp i kroppens immunförsvar, kunde vi utveckla en metod för att utröna en substans biologiska funktion. I denna modell visade sig **C38** partiellt *aktivera* AT_2R snarare än blockera AT_2R. En substans som partiellt aktiverar en receptor, kan vara mycket användbar då substansen ”normaliserar” receptorns aktivitet vilket skulle kunna vara mer effektivt i ett läkemedel än att blockera den.

De forskningsresultat som presenterats i denna avhandling har utökat vår förståelse för hur substansen **C38** interagerar med receptorn AT_2R. Med den kunskap som erhållits kan nya biologiska relevanta substanser designas, vilka kan användas för vidare studier av AT_2R och dess biologiska funktion.

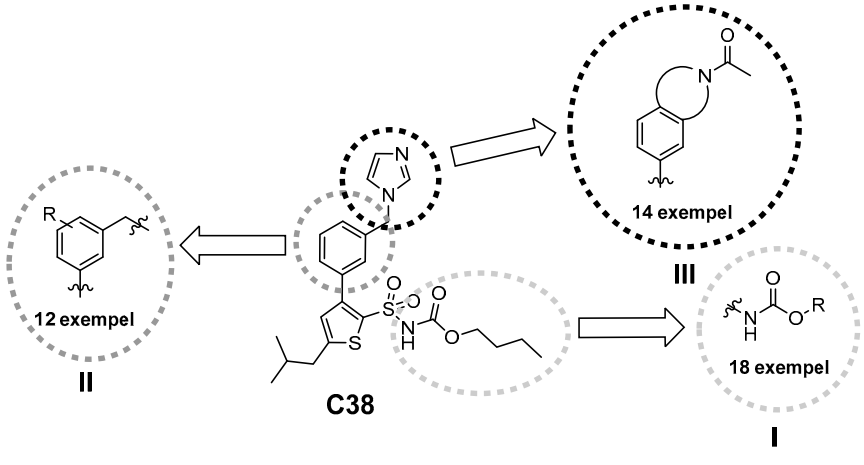

Figur 27. Startsubstansen C38 och de delar som undersöktes i denna avhandling.

Acknowledgments

First, I would like to extend my sincere gratitude to my main supervisor *Professor Mats Larhed*. I am thankful for the opportunity to join your research group as a PhD candidate, and for the support and encouragement you have given me in both science and non-science matters. I have had two excellent assistant supervisors in *Dr. Christian Sköld* and *Dr. Johan Gising*, thank you for your support, and your insightful and encouraging comments!

The work presented in this thesis is in many ways a collaborative effort and throughout the years, I have had the privilege to work with many talented and knowledgeable researchers. My heartfelt appreciation to all my collaborators and co-authors over the years, thank you for all your hard work and all our interesting discussions.

I am thankful to former and present colleagues at the Department of Medicinal Chemistry for contributing to a pleasant and productive work environment, filled with many laughs and plenty of interesting discussions on research, teaching, and much more.

I am grateful to *Professor Lars Fändriks* for welcoming me to his lab in Gothenburg and giving me the opportunity to learn from his group's extensive knowledge on the biological function of AT_2R. To all the members at gastlab: thank you for your warm hospitality that made me feel right at home. A special thank you to *Dr. Anna Casselbrant*, it has been an honor and a privilege to work with you.

I would also like to extend my deepest gratitude to *Professor emeritus Anders Hallberg* and *Dr. Charlotta Wallinder*, for sharing their experiences and knowledge of the AT_2R project.

Dr. Charles Hedgecock, my appreciation of the definite article might be low but my appreciation of you is high! Thank you for teaching me the ropes when I was new to the lab, and thank you for your critical review of this thesis. Any remaining inaccuracies are without doubt my own last minute revisions.

I would like to extend my sincere gratitude to *Uppsala University*, *Kjell och Märta Beijers Stiftelse*, *HF Sederholms Nordiska Stipendiestiftelse*, *IF Stiftelse för Farmacevtisk forskning*, *Elisabet och Alfred Ahlqvists Stiftelse*, and *John och Nils Ericssons Minnesfond* for providing financial support.

Last but foremost is of course my family. Thank you for always putting a smile on my face, for picking me up when I am down, for your unwavering support and patience, and for your endless love ♥

References

1. Hill, R. G. & Rang, H. P. *Drug Discovery & Development - Technology in Transition*. (Churchill Livingstone, 2013).
2. DiMasi, J. A., Grabowski, H. G. & Hansen, R. W. Innovation in the pharmaceutical industry: New estimates of R&D costs. *J. Health Econ.* **47,** 20–33 (2016).
3. de Laszlo, S. E. *et al.* A potent, orally active, balanced affinity angiotensin II AT1 antagonist and AT2 binding inhibitor. *J. Med. Chem.* **36,** 3207–3210 (1993).
4. Schacht, A. L. *et al.* How to improve R&D productivity: the pharmaceutical industry's grand challenge. *Nat. Rev. Drug Discov.* **9,** 203–214 (2010).
5. Mandrell, S. *et al.* An analysis of the attrition of drug candidates from four major pharmaceutical companies. *Nat. Rev. Drug Discov.* **14,** 475–486 (2015).
6. Hauser, A. S., Attwood, M. M., Rask-Andersen, M., Schiöth, H. B. & Gloriam, D. E. Trends in GPCR drug discovery: New agents, targets and indications. *Nat. Rev. Drug Discov.* **16,** 829–842 (2017).
7. Fredriksson, R. The G-Protein-Coupled Receptors in the Human Genome Form Five Main Families. Phylogenetic Analysis, Paralogon Groups, and Fingerprints. *Mol. Pharmacol.* **63,** 1256–1272 (2003).
8. Sato, J., Makita, N. & Iiri, T. Inverse agonism: the classic concept of GPCRs revisited. *Endocr. J.* **63,** 507–514 (2016).
9. Weis, W. I. & Kobilka, B. K. The Molecular Basis of G Protein–Coupled Receptor Activation. *Annu. Rev. Biochem.* **87,** 897–919 (2018).
10. Violin, J. D., Crombie, A. L., Soergel, D. G. & Lark, M. W. Biased ligands at G-protein-coupled receptors: Promise and progress. *Trends Pharmacol. Sci.* **35,** 308–316 (2014).
11. Wang, W., Qiao, Y. & Li, Z. New Insights into Modes of GPCR Activation. *Trends Pharmacol. Sci.* **39,** 367–386 (2018).
12. Katritch, V., Cherezov, V. & Stevens, R. C. Structure-Function of the G Protein–Coupled Receptor Superfamily. *Annu. Rev. Pharmacol. Toxicol.* **53,** 531–556 (2012).
13. Raizada, M. K., Philips, M. I. & Sumners, C. *Cellular and Molecular Biology of the Renin-Angiotensin System*. (CRC Press, 1993).
14. Tigerstedt, R. & Bergman, P. G. Niere und Kreislauf. *Scand. Acta Physiol.* **8,** 223–271 (1898).
15. Helmer, O. M. & Page, I. H. Purification and Some Properties of Renin. *J. Biol. Chem.* **127,** 757–763 (1939).
16. Skeggs, L. T., Kahn, J. R. & Shumway, N. P. The Preparation and Function of the Hypertensin-Converting Enzyme. *J. Exp. Med.* **72,** 295–299 (1956).
17. Skeggs, L. T., Lentz, K. E., Kahn, J. R., Shumway, N. P. & Woods, K. R. The Amino Acid Sequence of Hypertensin II. *J. Exp. Med.* **104,** 193–197 (1956).
18. Dinh, D. T., Frauman, A. G., Johnston, C. I. & Fabiani, M. E. Angiotensin receptors: distribution, signalling and function. *Clin. Sci.* **100,** 481–492 (2001).

19. Streeten, D. H. P., M.B., D. P., Anderson, G. H., Freiberg, J. M. & Dalakos, T. G. Use of an Angiotensin II Antagonist (Saralasin) in the Recognition of Angiotensinogenic Hypertension. *N. Engl. J. Med.* **292,** 657–662 (1975).
20. Streeten, D. H., Freiberg, J. M., Anderson, G. H. & Dalakos, T. G. Identification of angiotensinogenic hypertension in man using 1-sar-8-ala-angiotensin II (Saralasin, P-113). *Circ. Res.* **36,** 125–132 (1975).
21. Pettinger, W. A. & Mitchell, H. C. Renin Release, Saralasin and the Vasodilator-Beta-Blocker Drug Interaction in Man. *N. Engl. J. Med.* **292,** 1214–1217 (1975).
22. Unger, T., Steckelings, U. M. & Dzau, V. J. The Angiotensin AT2 Receptor: From Enigma to Therapeutic Target. in 1–10 (Academic Press, 2015).
23. Clark, M. T. & Pellmar, T. C. Design of Specific Inhibitors of Angiotensin-Converting Enzyme: New Class of Orally Active Antihypertensive Agents. *Science (80-.).* **195,** 441–444 (1977).
24. Brown, N. J. & Vaughan, D. E. Angiotensin-Converting Enzyme Inhibitors. *Circulation* **97,** 1411–1420 (1998).
25. Christ, D. D. *et al.* Losartan (DuP 753), An Orally Active Nonpeptide Angiotensin II Receptor Antagonist. *Cardiovasc. Drug Rev.* **9,** 317–339 (1991).
26. Burnier, M. & Brunner, H. R. Angiotensin II receptor antagonists. *Lancet* **355,** 637–645 (2000).
27. Pantzaris, N.-D., Karanikolas, E., Tsiotsios, K. & Velissaris, D. Renin Inhibition with Aliskiren: A Decade of Clinical Experience. *J. Clin. Med.* **6,** 61–80 (2017).
28. Shafiq, M. M., Menon, D. V. & Victor, R. G. Oral Direct Renin Inhibition: Premise, Promise, and Potential Limitations of a New Antihypertensive Drug. *Am. J. Med.* **121,** 265–271 (2008).
29. Whitebread, S., Mele, M., Kamber, B. & de Gasparo, M. Preliminary biochemical characterization of two angiotensin II receptor subtypes. *Biochem. Biophys. Res. Commun.* **163,** 284–291 (1989).
30. Chiu, A. T. *et al.* Identification of angiotensin II receptor subtypes. *Biochem. Biophys. Res. Commun.* **165,** 196–203 (1989).
31. de Gasparo, M., Whitebread, S., Criscione, L., Buehlmayer, P. & Furet, P. The AT2 Receptor: Historical Perspective. in *The Protective Arm of the Renin–Angiotensin System* 11–16 (Academic Press, 2015).
32. Apweiler, R. *et al.* Reorganizing the protein space at the Universal Protein Resource (UniProt). *Nucleic Acids Res.* **40,** 71–75 (2012).
33. Schiöth, H. B. & Lagerström, M. C. Structural diversity of g proteincoupled receptors and significance for drug discovery. *Nat. Rev. Drug Discov.* **7,** 339–357 (2008).
34. Koike, G. *et al.* Human Type 2 Angiotensin II Receptor Gene: Cloned, Mapped to the X Chromosome, and its mRNA is Expressed in the Human Lung. *Biochem. Biophys. Res. Commun.* **203,** 1842–1850 (1994).
35. Grady, E. F., Sechi, L. A., Griffin, C. A., Schambelan, M. & Kalinyak, J. E. Expression of AT2 Receptors in the Developing Rat Fetus. *J Clin Invest.* **88,** 921–933 (1991).
36. Bastien, N. R., Ciuffo, G. M., Saavedra, J. M. & Lambert, C. Angiotensin II receptor expression in the conduction system and arterial duct of neonatal and adult rat hearts. *Regul. Pept.* **63,** 9–16 (1996).
37. De Gasparo, M., Catt, K. J., Inagami, T., Wright, J. W. & Unger, T. International Union of Pharmacology. XXIII. The Angiotensin II Receptors. *Pharmacol. Rev.* **52,** 415–472 (2000).

38. AGT2R. *The Human Protein Atlas* (2018). Available at: https://www.proteinatlas.org/ENSG00000180772-AGTR2/tissue. (Accessed: 7th November 2018)
39. Steckelings, U. M. *et al.* The past, present and future of angiotensin II type 2 receptor stimulation. *Journal of the Renin-Angiotensin-Aldosterone System : JRAAS* **11,** 67–73 (2010).
40. Sumners, C., De Kloet, A. D., Krause, E. G., Unger, T. & Steckelings, U. M. Angiotensin type 2 receptors: Blood pressure regulation and end organ damage. *Curr Opin Pharmacol.* **21,** 115–121 (2015).
41. Nakajima, M. *et al.* The angiotensin II type 2 (AT2) receptor antagonizes the growth effects of the AT1 receptor: Gain-of-function study using gene transfer. *Proc. Natl. Acad. Sci.* **92,** 10663–10667 (1995).
42. Gallinat, S., Yu, M., Dorst, A., Unger, T. & Herdegen, T. Sciatic nerve transection evokes lasting up-regulation of angiotensin AT2 and AT1 receptor mRNA in adult rat dorsal root ganglia and sciatic nerves. *Mol. Brain Res.* **57,** 111–122 (1998).
43. Li, J. *et al.* Angiotensin AT2 receptor protects against cerebral ischemia-induced neuronal injury. *FASEB J.* **16,** 617–619 (2005).
44. Altarche-Xifro, W. *et al.* Cardiac c-kit+AT2+ Cell Population is Increased in Response to Ischemic Injury and Supports Cardiomyocyte Performance. *Stem Cells* **27,** 2488–2497 (2009).
45. Busche, S. *et al.* Expression of Angiotensin AT1 and AT2 Receptors in Adult Rat Cardiomyocytes after Myocardial Infarction. A Single-Cell Reverse Transcriptase-Polymerase Chain Reaction Study. *Am. J. Pathol.* **157,** 605–611 (2000).
46. Nio, Y., Matsubara, H., Murasawa, S., Kanasaki, M. & Inada, M. Regulation of Gene Transcription of Angiotensin 11 Receptor Subtypes in Myocardial Infarction. *Clin. Invest* **95,** 46–54 (1995).
47. Steckelings, U. M., Henz, B. M., Wiehstutz, S., Unger, T. & Artuc, M. Differential expression of angiotensin receptors in human cutaneous wound healing. *Br. J. Dermatol.* **153,** 887–893 (2005).
48. Oishi, Y. *et al.* Cardioprotective role of AT2 receptor in postinfarction left ventricular remodeling. *Hypertension* **41,** 814–818 (2003).
49. Sun, L. *et al.* Angiotensin II induces apoptosis in intestinal epithelial cells through the AT2 receptor, GATA-6 and the Bax pathway. *Biochem. Biophys. Res. Commun.* **424,** 663–668 (2012).
50. Wang, R. *et al.* Angiotensin II induces apoptosis in human and rat alveolar epithelial cells. *Am. J. Physiol.Lung Cell. Mol. Physiol* **275,** 1013–1017 (1998).
51. Yamada, T. *et al.* Angiotensin II Type 2 Receptor Mediates Vascular Smooth Muscle Cell Apoptosis and Antagonizes Angiotensin II Type 1 Receptor Action: An in Vitro Gene Transfer Study. *Pharmacol. Lett.* **63,** 289–295 (1998).
52. Suzuki, Y. *et al.* Inflammation and angiotensin II. *Int. J. Biochem. Cell Biol.* **35,** 881–900 (2003).
53. Mogi, M. & Horiuchi, M. Effect of angiotensin II type 2 receptor on stroke, cognitive impairment and neurodegenerative diseases. *Geriatr. Gerontol. Int.* **13,** 13–18 (2013).
54. Anand, U. *et al.* Angiotensin II type 2 receptor (AT2R) localization and antagonist-mediated inhibition of capsaicin responses and neurite outgrowth in human and rat sensory neurons. *Eur. J. Pain (United Kingdom)* **17,** 1012–1026 (2013).

55. Gallo-Payet, N. *et al.* Angiotensin II, a Neuropeptide at the Frontier between Endocrinology and Neuroscience: Is There a Link between the Angiotensin II Type 2 Receptor and Alzheimer's Disease? *Front. Endocrinol. (Lausanne).* **2,** 17 (2011).
56. Carey, R. M., Howell, N. L., Jin, X. H. & Siragy, H. M. Angiotensin type 2 receptor-mediated hypotension in angiotensin type-1 receptor-blocked rats. *Hypertension* **38,** 1272–1277 (2001).
57. Siragy, H. M., De Gasparo, M. & Carey, R. M. Angiotensin Type 2 Receptor Mediates Valsartan-Induced Hypotension in Conscious Rats. *Hypertension* **35,** 1074–1077 (2000).
58. Padia, S. H. & Carey, R. M. AT2 receptors: beneficial counter-regulatory role in cardiovascular and renal function. *Pflügers Arch. - Eur. J. Physiol.* **465,** 99–110 (2013).
59. Foulquier, S., Steckelings, U. M. & Unger, T. A tale of two receptors. *Nature* **493,** S9 (2013).
60. Willyard, C. As drug target reemerges, the question is to block or stimulate it. *Nat. Med.* **20,** 222–222 (2014).
61. Mitsubishi Tanabe Pharma Corporation. *Mitsubishi Tanabe Pharma*. (2017).
62. MOR107 | MorphoSys AG. Available at: https://www.morphosys.com/node/8165. (Accessed: 11th April 2019)
63. Wan, Y. *et al.* Design, synthesis, and biological evaluation of the first selective nonpeptide AT2 receptor agonist. *J. Med. Chem.* **47,** 5995–6008 (2004).
64. Horowitz, A. *et al.* The Selective Angiotensin II Type 2 Receptor Agonist, Compound 21, Attenuates the Progression of Lung Fibrosis and Pulmonary Hypertension in an Experimental Model of Bleomycin-Induced Lung Injury. *Front. Physiol.* **9,** 180 (2018).
65. Rice, A. S. C. *et al.* EMA401, an orally administered highly selective angiotensin II type 2 receptor antagonist, as a novel treatment for postherpetic neuralgia: A randomised, double-blind, placebo-controlled phase 2 clinical trial. *Lancet* **383,** 1637–1647 (2014).
66. Smith, M. T., Wyse, B. D. & Edwards, S. R. Small molecule angiotensin II type 2 receptor (AT2R) antagonists as novel analgesics for neuropathic pain: comparative pharmacokinetics, radioligand binding, and efficacy in rats. *Pain Med.* **14,** 692–705 (2013).
67. Rice, A. S. C. & Smith, M. T. Angiotensin II Type 2-Receptor: New clinically validated target in the treatment of neuropathic pain. *Clin. Pharmacol. Ther.* **97,** 128–130 (2015).
68. Kivlighn, S. D. *et al.* Discovery of L-162,313: a nonpeptide that mimics the biological actions of angiotensin II. *Am. J. Physiol.* **268,** R820–R823 (1995).
69. Murugaiah, A. M. S. *et al.* From the first selective non-peptide AT(2) receptor agonist to structurally related antagonists. *J. Med. Chem.* **55,** 2265–78 (2012).
70. Wannberg, J. *et al.* A convenient transesterification method for synthesis of AT2 receptor ligands with improved stability in human liver microsomes. *Bioorg. Med. Chem. Lett.* **28,** 519–522 (2018).
71. Blankley, C. J. *et al.* Synthesis and Structure-Activity Relationships of a Novel Series of Non-Peptide Angiotensin II Receptor Binding Inhibitors Specific for the AT2 Subtype. *J. Med. Chem.* **34,** 3248–3260 (1991).
72. VanAtten, M. K. *et al.* A Novel Series of Selective, Non-Peptide Inhibitors of Angiotensin II Binding to the AT2 Site. *J. Med. Chem.* **36,** 3985–3992 (1993).
73. Mantlo, N. B. *et al.* Imidazo[4,5-b]pyridine-based AT1 / AT2 angiotensin II receptor antagonists. *Bioorg. Med. Chem. Lett.* **4,** 17–22 (1994).

74. Dudley, D. T. *et al.* Subclasses of Angiotensin II Binding Sites and Their Functional Significance. *Mol. Pharmacol.* **38,** 370–377 (1990).
75. Baron, R., Binder, A. & Wasner, G. Neuropathic pain: diagnosis, pathophysiological mechanisms, and treatment. *Lancet Neurol.* **9,** 807–819 (2010).
76. Van Hecke, O., Austin, S. K., Khan, R. A., Smith, B. H. & Torrance, N. Neuropathic pain in the general population: A systematic review of epidemiological studies. *Pain* **155,** 654–662 (2014).
77. Colloca, L. *et al.* Neuropathic pain. *Nat. Rev. Dis. Prim.* **3,** 17002 (2017).
78. Davies, M., Brophy, S., Williams, R. & Taylor, A. The Prevalence, Severity, and Impact of Painful Diabetic Peripheral Neuropathy in Type 2 Diabetes. *Diabetes Care* **29,** 1518–1522 (2006).
79. Daousi, C. *et al.* Chronic painful peripheral neuropathy in an urban community: a controlled comparison of people with and without diabetes. *Diabet. Med.* **21,** 976–982 (2004).
80. Woolf, C. J. Neuropathic pain: aetiology, symptoms, mechanisms, and managment. *Lancet* **353,** 1959–1964 (1999).
81. Beniczky, S., Tajti, J., Tímea Varga, E. & Vécsei, L. Evidence-based pharmacological treatment of neuropathic pain syndromes Review. *J Neural Transm* **112,** 735–749 (2005).
82. Chakrabarty, A., Blacklock, A., Svojanovsky, S. & Smith, P. G. Estrogen Elicits Dorsal Root Ganglion Axon Sprouting via a Renin-Angiotensin System. *Endocrinology* **149,** 3452–3460 (2008).
83. Gendron, L. *et al.* Signals from the AT2 (Angiotensin Type 2) Receptor of Angiotensin II Inhibit p21 ras and Activate MAPK (Mitogen-Activated Protein Kinase) to Induce Morphological Neuronal Differentiation in NG108–15 Cells. *Mol. Endocrinol.* **13,** 1615–1626 (1999).
84. Kang, J., Sumners, C. & Posner, P. Modulation of net outward current in cultured neurons by angiotensin II: involvement of AT1 and AT2 receptors. *Brain Res.* **580,** 317–324 (1992).
85. Keppel Hesselink, J. M. & Schatman, M. E. EMA401: an old antagonist of the AT2R for a new indication in neuropathic pain. *J. Pain Res.* **10,** 439–443 (2017).
86. Alenina, N. & dos Santos, R. A. S. Angiotensin(1-7) and Mas: A Brief History. in *The Protective Arm of the Renin– Angiotensin System* 155–159 (Academic Press, 2015).
87. Young, D., Waitches, G., Birchmeier, C., Fasano, O. & Wigler, M. Isolation and characterization of a new cellular oncogene encoding a protein with multiple potential transmembrane domains. *Cell* **45,** 711–719 (1986).
88. Santos, R. A. S. *et al.* Angiotensin-(1-7) is an endogenous ligand for the G protein-coupled receptor Mas. *Proc. Natl. Acad. Sci.* **100,** 8258–8263 (2003).
89. Simões e Silva, A. C., Silveira, K. D., Ferreira, A. J. & Teixeira, M. M. ACE2, angiotensin-(1-7) and Mas receptor axis in inflammation and fibrosis. *Br. J. Pharmacol.* **169,** 477–492 (2013).
90. Perlman, S. *et al.* Non-peptide Angiotensin Agonist. Functional and Molecular Interaction with the AT1 Receptor. *J. Biol. Chem.* **270,** 1493–1496 (1995).
91. Wan, Y. *et al.* First reported nonpeptide AT1 receptor agonist (L-162,313) acts as an AT2 receptor agonist in vivo. *J. Med. Chem.* **47,** 1536–1546 (2004).
92. Larhed, M., Hallberg, M. & Hallberg, A. Nonpeptide AT2R agonists. *Med. Chem. Rev.* **51,** 69–82 (2016).
93. Steckelings, U. M. *et al.* Non-peptide AT2-receptor agonists. *Curr. Opin. Pharmacol.* **11,** 187–192 (2011).

94. Alterman, M. Development of selective non-peptide angiotensin II type 2 receptor agonists. *J. Renin. Angiotensin. Aldosterone. Syst.* **11,** 57–66 (2010).
95. Wu, X. *et al.* Selective angiotensin II AT2 receptor agonists: arylbenzylimidazole structure-activity relationships. *J. Med. Chem.* **49,** 7160–7168 (2006).
96. Murugaiah, A. M. S. *et al.* Selective angiotensin II AT(2) receptor agonists devoid of the imidazole ring system. *Bioorg. Med. Chem.* **15,** 7166–7183 (2007).
97. Mahalingam, A. K. *et al.* Selective angiotensin II AT(2) receptor agonists with reduced CYP 450 inhibition. *Bioorg. Med. Chem.* **18,** 4570–4590 (2010).
98. Wallinder, C. *et al.* Selective angiotensin II AT2 receptor agonists: Benzamide structure-activity relationships. *Bioorg. Med. Chem.* **16,** 6841–6849 (2008).
99. Guimond, M.-O., Wallinder, C., Alterman, M., Hallberg, A. & Gallo-Payet, N. Comparative functional properties of two structurally similar selective nonpeptide drug-like ligands for the angiotensin II type-2 (AT 2) receptor. Effects on neurite outgrowth in NG108-15 cells. *Eur. J. Pharmacol.* **699,** 160–171 (2013).
100. Wallinder, C. *et al.* Interconversion of Functional Activity by Minor Structural Alterations in Nonpeptide AT2 Receptor Ligands. *ACS Med. Chem. Lett.* **6,** 178–182 (2015).
101. Khosla, M. C. *et al.* Synthesis of Some Analogs of Angiotensin II as Specific Antagonists of the Parent Hormone. *J. Med. Chem.* **15,** 792–795 (1972).
102. Perlman, S. *et al.* Dual agonistic and antagonistic property of nonpeptide angiotensin AT1 ligands: susceptibility to receptor mutations. *Mol. Pharmacol.* **51,** 301–11 (1997).
103. Taylor, L. D., Pluhar, M. & Rubin, L. E. Reaction of sulfonyl isocyanates with polymeric alcohols to produce a polymeric acid. *J. Polym. Sci. Part B Polym. Lett.* **5,** 77–78 (1967).
104. Taylor, L. D., MacDonald, R. J. & Rubin, L. E. Acidity and stability of sulfonyl carbamates and ureas. *J. Polym. Sci. Part A-1 Polym. Chem.* **9,** 3059–3061 (1971).
105. Hallberg, M., Sumners, C., Steckelings, U. M. & Hallberg, A. Small-molecule AT2 receptor agonists. *Med. Res. Rev.* **38,** 602–624 (2018).
106. Hirama, M., Iwashita, M., Yamazakib, Y. & Ito, S. *Carbamate Mediated Functionalization of Unsaturated Alcohols II. Regio- and Stere-Selective Synthesis of 1,3-Syn and 1,2-Anti Amino Alcohol Derviatives via Iodocarbamation*. *Tetrahedron Letters* **25,** (1984).
107. Larhed, M. & Hallberg, A. Microwave-assisted high-speed chemistry: a new technique in drug discovery. *Drug Discov. Today* **6,** 406–416 (2001).
108. Lidström, P., Tierney, J., Wathey, B. & Westman, J. Microwave assisted organic synthesis - a review. *Tetrahedron* **57,** 9225–9283 (2001).
109. Kappe, C. O. & Dallinger, D. The impact of microwave synthesis on drug discovery. *Nat. Rev. Drug Discov.* **5,** 51–63 (2006).
110. Mingos, D. M. P. & Baghurst, D. R. Applications of Microwave Dielectric Heating Effects to Synthetic Problems in Chemistry. *Chem. Soc. Rev.* **20,** 1–47 (1991).
111. Kappe, C. O. Synthetic Methods Controlled Microwave Heating in Modern Organic Synthesis. *Angew. Chem. Int. Ed* **43,** 6250–6284 (2004).
112. Caddick, S. & Fitzmaurice, R. Microwave enhanced synthesis. *Tetrahedron* **65,** 3325–3355 (2009).

113. Wathey, B., Tierney, J., Lidström, P. & Westman, J. The impact of microwave-assisted organic chemistry on drug discovery. *Drug Discov. Today* **7,** 373–380 (2002).
114. Gising, J., Odell, L. R. & Larhed, M. Microwave-assisted synthesis of small molecules targeting the infectious diseases tuberculosis, HIV/AIDS, malaria and hepatitis C. *Org. Biomol. Chem.* **10,** 2713–2729 (2012).
115. de la Hoz, A. & Loupy, A. *Microwaves in Organic Synthesis*. (Wiley-VCH Verlag GmbH & Co. KGaA, 2013). doi:10.1002/9783527651313
116. Malet-Sanz, L. & Susanne, F. Continuous Flow Synthesis. A Pharma Perspective. *J. Med. Chem.* **55,** 4062–4098 (2012).
117. Gutmann, B., Cantillo, D. & Kappe, C. O. Continuous-flow technology - A tool for the safe manufacturing of active pharmaceutical ingredients. *Angew. Chemie - Int. Ed.* **54,** 6688–6728 (2015).
118. Wiles, C. & Watts, P. Continuous process technology: A tool for sustainable production. *Green Chem.* **16,** 55–62 (2014).
119. Anderson, N. G. Using continuous processes to increase production. *Org. Process Res. Dev.* **16,** 852–869 (2012).
120. Bagley, M. C., Jenkins, R. L., Lubinu, M. C., Mason, C. & Wood, R. A simple continuous flow microwave reactor. *J. Org. Chem.* **70,** 7003–7006 (2005).
121. Wilson, N. S., Sarko, C. R. & Roth, G. P. Development and applications of a practical continuous flow microwave cell. *Org. Process Res. Dev.* **8,** 535–538 (2004).
122. He, P., Haswell, S. J. & Fletcher, P. D. I. Microwave-assisted Suzuki reactions in a continuous flow capillary reactor. *Appl. Catal. A Gen.* **274,** 111–114 (2004).
123. Shore, G., Morin, S. & Organ, M. G. Catalysis in capillaries by Pd thin films using Microwave-Assisted Continuous-flow Organic Synthesis (MACOS). *Angew. Chemie - Int. Ed.* **45,** 2761–2766 (2006).
124. Morschhäuser, R. *et al.* Microwave-assisted continuous flow synthesis on industrial scale. *Green Process. Synth.* **1,** 281–290 (2012).
125. Bremner, W. S. & Organ, M. G. Multicomponent reactions to form heterocycles by microwave-assisted continuous flow organic synthesis. *J. Comb. Chem.* **9,** 14–16 (2007).
126. Glasnov, T. N. & Kappe, C. O. Microwave-assisted synthesis under continuous-flow conditions. *Macromol. Rapid Commun.* **28,** 395–410 (2007).
127. Comer, E. & Organ, M. G. A microreactor for microwave-assisted capillary (continuous flow) organic synthesis. *J. Am. Chem. Soc.* **127,** 8160–8167 (2005).
128. Smith, C. J., Iglesias-Sigüenza, F. J., Baxendale, I. R. & Ley, S. V. Flow and batch mode focused microwave synthesis of 5-amino-4-cyanopyrazoles and their further conversion to 4-aminopyrazolopyrimidines. *Org. Biomol. Chem.* **5,** 2758–2761 (2007).
129. Öhrngren, P. *et al.* Evaluation of a Nonresonant Microwave Applicator for Continuous- Flow Chemistry Applications. *Org. Process Res. Dev.* **16,** 1053–1063 (2012).
130. Rydfjord, J. *et al.* Decarboxylative palladium(II)-catalyzed synthesis of aryl amidines from aryl carboxylic acids: Development and mechanistic investigation. *Chem. - A Eur. J.* **19,** 13803–13810 (2013).
131. Rydfjord, J. *et al.* Temperature measurements with two different IR sensors in a continuous-flow microwave heated system. *Beilstein J. Org. Chem.* **9,** 2079–2087 (2013).

132. Behrends, M. *et al.* N -Aryl Isoleucine Derivatives as Angiotensin II AT 2 Receptor Ligands. *ChemistryOpen* **3,** 65–75 (2014).
133. Zhang, H. *et al.* Structural basis for selectivity and diversity in angiotensin II receptors. *Nature* **544,** 327–332 (2017).
134. Zhang, H. *et al.* Structure of the Angiotensin Receptor Revealed by Serial Femtosecond Crystallography. *Cell* **161,** 833–844 (2015).
135. Asada, H. *et al.* Crystal structure of the human angiotensin II type 2 receptor bound to an angiotensin II analog. *Nat. Struct. Mol. Biol.* **25,** 1–9 (2018).
136. Kevin, N. J., Rivero, R. A., Greenlee, W. J., Chang, R. S. L. & Chen, T. B. Subtituted phenylthiophene benzoylsulfonamides with potent binding affinity to angiotensin II AT1 and AT2 receptors. *Bioorg. Med. Chem. Lett.* **4,** 189–194 (1994).
137. Gillis, E. P. & Burke, M. D. A Simple and Modular Strategy for Small Molecule Synthesis: Iterative Suzuki-Miyaura Coupling of B-Protected Haloboronic Acid Building Blocks. *J. Am. Chem. Soc* **129,** 6716–6717 (2007).
138. Park, B. K., Kitteringham, N. R. & O 'neill, P. M. Metabolism of fluorine-containing drugs. *Annu. Rev. Pharmacol. Toxicol* **41,** 443–470 (2001).
139. Müller, K., Faeh, C. & Diederich, F. Fluorine in pharmaceuticals: looking beyond intuition. *Science (80-.).* **317,** 1881–1886 (2007).
140. Zhang, H. *et al.* Structural Basis for Ligand Recognition and Functional Selectivity at Angiotensin Receptor *. *J. Biol. Chem.* **290,** 29127–29139 (2015).
141. Poulos, T. L. & Howard, A. J. Crystal Structures of Metyrapone- and Phenylimidazole-Inhibited Complexes of Cytochrome P-450. *Biochemistry* **26,** 8165–8174 (1987).
142. Kerns, E. H. & Di, L. Cytochrome P450 Inhibition. in *Drug-like Properties: Concepts, Structure Design and Methods from ADME to Toxicity Optimization* 197–208 (Academic Press, 2008).
143. Mahalingam, A. K. *et al.* Selective angiotensin II AT2 receptor agonists with reduced CYP 450 inhibition. *Bioorganic Med. Chem.* **18,** 4570–4590 (2010).
144. Ulysse, L. G. *et al.* Process Development and Pilot-Scale Synthesis of New Cyclization Conditions of Substituted Phenylacetamides to Tetrahydroisoquinoline-2-ones Using Eaton's Reagent. *Org. Process Res. Dev.* **14,** 225–228 (2010).
145. Eaton, P. E., Carlson, G. R. & Lee, J. T. Phosphorus Pentoxide-Methanesulfonic Acid. A Convenient Alternative to Polyphosphoric Acid. *J. Org. Chem* **38,** 4071–4073 (1973).
146. Johansson, B. *et al.* Angiotensin II type 2 receptor-mediated duodenal mucosal alkaline secretion in the rat. *Am. J. Physiol. Gastrointest. Liver Physiol.* **280,** G1254–G1260 (2001).
147. Buisson, B., Bottari, S. P., de Gasparo, M., Gallo-Payet, N. & Payet, M. D. The angiotensin AT2 receptor modulates T-type calcium current in non-differentiated NG108-15 cells. *Fed. Eur. Biochem. Soc.* **309,** 161–164 (1992).
148. Gendron, L., Payet, M. D. & Gallo-Payet, N. The angiotensin type 2 receptor of angiotensin II and neuronal differentiation: from observations to mechanisms. *J. Mol. Endocrinol.* **31,** 359–372 (2003).
149. Laflamme, L., De Gasparo, M., Gallo, J.-M., Payet, M. D. & Gallo-Payet, N. Angiotensin II Induction of Neurite Outgrowth by AT 2 Receptors in NG108-15 Cells. *J. Biol. Chem.* **271,** 22729–22735 (1996).
150. Georgsson, J. *et al.* Synthesis of a New Class of Druglike Angiotensin II C-Terminal Mimics with Affinity for the AT 2 Receptor. *J. Med. Chem.* **50,** 1711–1715 (2007).

151. Gordon, S. & Taylor, P. R. Monocyte and macrophage heterogeneity. *Nat. Rev. Immunol.* **5,** 953–964 (2005).
152. Wynn, T. A., Chawla, A. & Pollard, J. W. Macrophage biology in development, homeostasis and disease. *Nature* **496,** 445–455 (2013).
153. Sica, A. & Mantovani, A. Macrophage plasticity and polarization : in vivo veritas. *J. Clin. Invest.* **122,** 787–795 (2012).
154. Menk, M. *et al.* Stimulation of the Angiotensin II AT2 Receptor is Anti-inflammatory in Human Lipopolysaccharide-Activated Monocytic Cells. *Inflammation* **38,** 1690–1699 (2015).
155. Rompe, F. *et al.* Direct angiotensin II type 2 receptor stimulation acts anti-inflammatory through epoxyeicosatrienoic acid and inhibition of nuclear factor κB. *Hypertension* **55,** 924–931 (2010).
156. Dhande, I., Ma, W. & Hussain, T. Angiotensin AT2 receptor stimulation is anti-inflammatory in lipopolysaccharide-activated THP-1 macrophages via increased interleukin-10 production. *Hypertens. Res.* **38,** 21–29 (2015).
157. Guo, F. *et al.* Role of Angiotensin II Type 1 Receptor in Angiotensin II-Induced Cytokine Production in Macrophages. *J. Interf. Cytokine Res.* **31,** 351–361 (2011).
158. Taciak, B. *et al.* Evaluation of phenotypic and functional stability of RAW 264.7 cell line through serial passages. *PLoS One* **13,** e0198943 (2018).
159. Peluso, A. A. *et al.* Identification of protein phosphatase involvement in the AT 2 receptor-induced activation of endothelial nitric oxide synthase. *Clin. Sci.* **132,** 777–790 (2018).
160. Bosnyak, S. *et al.* Relative affinity of angiotensin peptides and novel ligands at AT 1 and AT 2 receptors. *Clin. Sci.* **121,** 297–303 (2011).
161. Villela, D. *et al.* Angiotensin type 2 receptor (AT2R) and receptor Mas: a complex liaison. *Clin. Sci.* **128,** 227–234 (2015).
162. Leonhardt, J. *et al.* Evidence for Heterodimerization and Functional Interaction of the Angiotensin Type 2 Receptor and the Receptor MAS. *Hypertension* **69,** 1128–1135 (2017).
163. Kostenis, E. *et al.* G-Protein–Coupled Receptor Mas Is a Physiological Antagonist of the Angiotensin II Type 1 Receptor. *Circulation* **111,** 1806–1813 (2005).
164. AbdAlla, S., Lother, H., Abdel-tawab, A. M. & Quitterer, U. The Angiotensin II AT2 Receptor Is an AT1 Receptor Antagonist. *J. Biol. Chem.* **276,** 39721–39726 (2001).
165. Sampson, A. K. *et al.* Compound 21, a selective agonist of angiotensin AT2 receptors, prevents endothelial inflammation and leukocyte adhesion in vitro and in vivo. *Br. J. Pharmacol.* **173,** 729–740 (2016).
166. Shepherd, A. J. *et al.* Macrophage angiotensin II type 2 receptor triggers neuropathic pain. *Proc. Natl. Acad. Sci.* **115,** 201721815 (2018).
167. Shepherd, A. J. *et al.* Angiotensin II Triggers Peripheral Macrophage-to-Sensory Neuron Redox Crosstalk to Elicit Pain. *J. Neurosci.* **32,** 7032–7057 (2018).

Acta Universitatis Upsaliensis

Digital Comprehensive Summaries of Uppsala Dissertations from the Faculty of Pharmacy 269

Editor: The Dean of the Faculty of Pharmacy

A doctoral dissertation from the Faculty of Pharmacy, Uppsala University, is usually a summary of a number of papers. A few copies of the complete dissertation are kept at major Swedish research libraries, while the summary alone is distributed internationally through the series Digital Comprehensive Summaries of Uppsala Dissertations from the Faculty of Pharmacy. (Prior to January, 2005, the series was published under the title "Comprehensive Summaries of Uppsala Dissertations from the Faculty of Pharmacy".)

Distribution: publications.uu.se
urn:nbn:se:uu:diva-381102

ACTA
UNIVERSITATIS
UPSALIENSIS
UPPSALA
2019